Physical properties of near-Earth asteroids

D. F. Lupishko[1] and M. Di Martino[2]

[1] Astronomical Observatory of Kharkov State University, Sumskaya str. 35, Kharkov 310022, Ukraine
[2] Osservatorio Astronomico di Torino, I-10025 Pino Torinese (TO), Italy

Abstract. More than 400 near–Earth asteroids (NEAs) have been discovered and their discovery rate is continuously increasing. The study of the physical properties of these objects is necessary in order to understand their history and relations with comets and meteors, for the analysis and solution of new applied topics, such as the asteroid hazard problem, and the possibility of using NEAs as future sources of raw materials in near-Earth space. The present review article collects and summarizes the most important new data on the physical properties of Earth-approaching asteroids, obtained by photometric, polarimetric, spectroscopic, radar and other techniques. The analysis of all the available data gives clear indications that asteroid main-belt is the main source of NEAs. © 1998 Elsevier Science Ltd. All rights reserved

"We are now on the threshold of a new era of asteroid studies"
Tom Gehrels
(Physical Studies of Minor Planets. 1971, p. vii)

1. Introduction

Almost one century has passed since the discovery of the first near-Earth asteroid (NEA), 433 Eros. This object was discovered on 13 August 1898 by the German amateur astronomer Gustav Witt in Berlin and, independently, by Auguste Charlois in Nice, France. Since then, several hundreds of new objects from this population have been detected and new data on their dynamical, physical and mineralogical properties has been collected. From these data the main differences between NEAs and main-belt asteroids (MBAs) can be analyzed. Observable NEAs are

rather small objects, usually of the order of a few kilometres or less. MBAs of such sizes are generally not accessible to ground-based observations. Therefore, when NEAs approach the Earth (at distances which can be as small as 0.01–0.02 AU and sometimes less) they give a unique chance to study objects of such small sizes. Some of them possibly represent primordial matter, which has preserved a record of the earliest stages of the Solar System evolution, while the majority are fragments coming from catastrophic collisions that occurred in the asteroid main-belt and could provide "a look" at the interior of their much larger parent bodies.

Therefore, NEAs are objects of special interest for several reasons. First, from the point of view of fundamental science, the problems raised by their origin in planet-crossing orbits, their life-time, their possible genetic relations with comets and meteorites, etc. are closely connected with the solution of the major problem of planetary science of the origin and evolution of the Solar System.

Secondly, the applied aspects of NEA studies are becoming more and more evident due to the critical importance they may have for the continuation of civilization. These objects are also believed to be potential sources of metals and other raw materials in near-Earth space. As is evidenced from meteoritic data, some of the Earth-approaching asteroids contain volatile compounds (hydrogen, nitrogen, carbon, oxygen, organics) over 100 times more abundant than in the most volatile-rich lunar materials. Moreover, observational data suggest that among NEAs there are pure metallic objects. The Sikhote–Alinskij meteorite, consisting of 94% Fe and 6% Ni (found in the far East of Siberia in 1947), is an indirect confirmation of this.

Finally, the third aspect of the importance of NEA research is related to the asteroid hazard problem. According to the available estimates, there are about 1500 asteroids larger than 1 km diameter, and about 135,000 larger than 100 m which cross the Earth's orbit. The collision of any of them with the Earth would be catastrophic on a local or global scale. The main problem is that the orbits of approximately 7% of the Earth-crossers

---

Correspondence to: Mario Di Martino. E-mail: dimartino@to.astro.it; Tel.: 39-11-8101935; Fax: 30-11-8101930

larger than 1 km in diameter, and much less of the smaller ones. is known today. In order to protect mankind against the hazard connected with asteroid and comet impacts on the Earth, the study of the physical properties of these objects is of fundamental importance.

The last detailed review on physical and mineralogical properties of NEAs was published by McFadden *et al.* (1989). Now the number of discovered NEAs has increased more than 3-fold and new data on their orbital properties, shapes, mineralogy, etc. have been obtained during recent years. The aim of this paper is to collect and summarize all the relevant information available today for these objects.

2. The groups and total number of NEAs

According to their present osculating orbital elements. NEAs have been conventionally classified in three groups : Atens, Apollos and Amors (Shoemaker *et al.*, 1979). Aten asteroids have orbits which lie inside that of the Earth, with semimajor axis a and aphelion distances Q satisfying the relations :

$$a < 1\,\text{AU}, \quad Q \geqslant 0.983\,\text{AU},$$

thus overlapping Earth's orbit in the region of their aphelia, as $Q = 0.983$ corresponds to the present perihelion of the Earth.

Apollo-asteroids are defined according to the condition :

$$a \geqslant 1\,\text{AU}, \quad q \leqslant 1.017\,\text{AU}$$

(1.017 AU being the aphelion distance of the Earth), therefore they overlap Earth's orbit near their perihelia. Thus, both Atens and Apollos overlap the orbit of the Earth with a period shorter (Aten-group) or longer (Apollo-group) than 1 year. They are also called Earth-crossing asteroids (ECAs).

Amor-asteroids have orbits with current perihelion distances greater then the aphelion distance of the Earth. For them :

$$a \geqslant 1\,\text{AU}, \quad 1.017 < q \leqslant 1.3\,\text{AU}.$$

As a consequence, Amors usually do not overlap Earth's orbit; they can only approach it. But secular variations of the eccentricities and semimajor axes of Amor-group objects lead to a part-time orbital overlap with Earth's orbit, and conversely, some Apollo-asteroids lose the overlap with the Earth and become Amors for a certain period of time (Shoemaker *et al.*, 1990). According to Rabinowitz *et al.* (1994a), about 50% of the asteroids currently classified as Amors are ECAs, while a small number of Apollos are not Earth-crossing, because their orbits do not intersect the Earth's orbit at present.

Milani *et al.* (1989), from the analysis of the orbital evolution of a sample of 89 Earth-crossing and almost-crossing asteroids over a time span of 200,000 years, divided these objects into six well-defined classes of dynamical behavior, named after the best-known, most representative object in each class: Geographos, Toro, Alinda, Kozai, Oljato, and Eros. This classification is indicative of long-term behavior and, of course, differs from the Aten–Apollo–Amor, based only upon the osculating orbital elements.

During the first years of the *Spacewatch Program* operation, the observations carried out with the 0.91 m telescope of the University of Arizona at Kitt Peak found evidences of an excess of very small near-Earth objects (5 50 m) with orbital elements similar to the Earth's (Rabinowitz *et al.*, 1993). Analysing these data Rabinowitz (1994) suggested that two distinct populations of NEAs exist. One of them corresponds to the traditional Aten, Apollo and Amor groups, while the other, composed by small objects less than 50 m in size, is characterized by low eccentricities and inclinations, and semi-major axis ~ 1 AU. This population forms a previously unknown asteroid concentration near the Earth's orbit (the so-called "near-Earth asteroid belt") with perihelia between 0.9 and 1.1 AU and aphelia < 1.4 AU. At absolute magnitude $H = 29$ the relative number of these objects is 40 times larger (to within a factor of 2) than a power law extrapolation of the magnitude frequency of km-sized ECAs (Rabinowitz, 1994).

The Minor Planet Center list of discovered NEAs, updated at May, 1997, contained 409 objects (24 Atens, 194 Apollos and 191 Amors). The estimates of the total number of ECAs, that is Atens, Apollos and Earth-crossing Amors, as a function of their diameters (Rabinowitz *et al.*, 1994a), give about 20 asteroids larger than 5 km in diameter (but only 12 objects of such sizes are presently known), 1500 larger than 1 km, and about 135,000 larger than 100 m (see Fig. 1, taken from Rabinowitz *et al.*, 1994a). The total number of NEAs (not only ECAs) is approximately 1.25 times larger. ECA population consists of 10% of Atens, 65% of Apollos and 25% of Earth-crossing Amors (Morrison, 1992). One of the most recent estimates gives an overall number of km-sized NEAs of the order of 2000 and more than one million of 100 m sized bodies (Menichella *et al.*, 1996).

The population of NEAs can be approximated by a power law, which reflects a general exponential increase of the number of asteroids as we go to smaller sizes :

$$n = kD^{\,b},$$

where : n is the number of asteroids larger than a given diameter D, k is the constant and b is the power-law exponent. However, it was shown that a better approximation can be obtained by using three different power-law exponents in three different diameter ranges (Rabinowitz *et al.*, 1994a).

Discovery completeness of ECAs naturally depends on asteroid absolute magnitude H, hence on diameter and albedo. Table 1 shows the estimated completeness of discovered ECAs, according to Rabinowitz *et al.* (1994a). Discovery is thought to be complete up to $H = 13.2$ mag. In term of size, this means that all ECAs larger than 12 km, in the case of low-albedo asteroids (C-class), and larger than 6 km for moderate-albedo objects (S-class) have been detected. About 35% of ECAs brighter than 15.0 mag (6 km and 3 km in size, respectively) also should have been discovered. But only about 15% of Earth-crossers brighter than 16.0 mag (4 km and 2 km) and only about 7% of objects with diameters of 2 km and 1 km are known today. As it was already mentioned, this is the
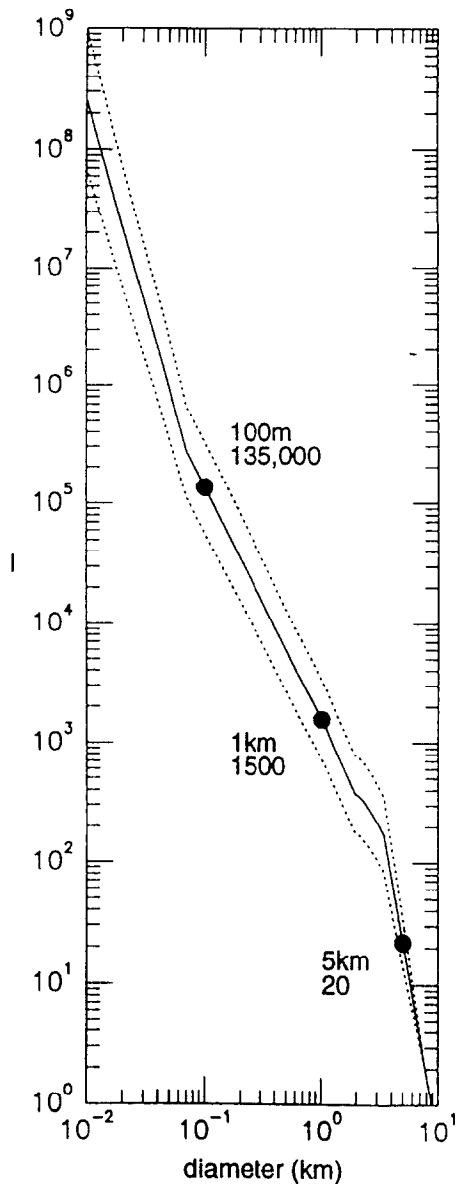
Fig. 1. Estimated number of Earth-crossing asteroids larger than a given diameter (Rabinowitz *et al.*, 1994a)

Table 1. Completeness of discovered ECAs

Absolute mag. (brighter than)	Diameter (km)	Completeness (%)
13.2	12 ÷ 6	100
15.0	6 ÷ 3	35
16.0	4 ÷ 2	15
17.7	2 ÷ 1	7

most critical deficiency to be solved in the framework of the asteroid hazard problem.

3. Taxonomic classification

The most complete data-set on NEA taxonomy previously published has been provided by Chapman *et al.* (1994).

Supplemented by the most recent data (Xu *et al.*, 1995; Di Martino *et al.*, 1995; and others), it shows that only 69 asteroids of the near-Earth population have been classified. Moreover, for 11 of them the classification is still ambiguous.

Figure 2 shows that among classified NEAs practically all taxonomic classes are present, with the exception of B and maybe P and T classes. these are low-albedo classes, whose location is mainly in the outer part of the main-belt. One of the important results of NEA taxonomy, compared with that of MBAs, is a quite different relative abundance of the two most populous classes, C and S. About one half of the classified NEAs belong to the S class, while in the main-belt the low albedos asteroids (C-class and its subclasses, B, F, G) predominate. Available data show that among NEAs the number of S-type objects exceeds that of low albedo types by as much as a factor of three. By contrast, among the MBAs the ratio is inverse, about 1 : 5 (Zellner, 1979).

It is widely suspected that the observed overabundance of S-type objects in the NEA population is a result of observational selection effects. Therefore, one of the main questions of NEA taxonomy is the real ratio of C and S asteroids approaching the Earth. The limiting magnitude of an asteroid, which can be detected by a magnitude-limited survey at given geocentric and heliocentric distances, is a function of its albedo, diameter and solar phase angle. So, three principal factors determining the observational selection effects are responsible for the apparent overabundance of S-type objects among NEAs: albedo, size distribution and larger phase function darkening of C-objects with respect to S ones. Among these factors the first two are dominant.

Tedesco and Gradie (1987) took into consideration only albedo bias (the main factor). They found a similarity in the relative abundances of classes C, S and M among 38 NEAs (for which such classes were available) and inner asteroid belt (between the 3 : 1 and 5 : 2 resonances, i.e. between 2.50 and 2.82 AU).

Luu and Jewitt (1989) applied a Monte Carlo approach to model the selection effects in observations of both NEAs and MBAs, in order to compare the respective bias effects. Their models took into account not only albedo differences between C and S asteroids but also asteroid size distributions and the larger phase-function darkening of C-types with respect to S-types (due to the difference in phase coefficients of their magnitude–phase dependences). MBAs are not so much affected by phase darkening as NEAs, because of their comparatively small values of phase angles. The results of modelling allowed Luu and Jewitt to conclude that: (a) the obtained bias factor B(S:C) for NEAs is in the range 5 < B(S:C) < 6 and is large enough to account for the observed overabundance of S-types among NEAs; (b) NEA bias factor is larger than that for MBAs because NEAs are discovered at larger phase angles than MBAs, and hence suffer more from differential phase darkening; (c) there is no compelling observational evidence for a difference in the ratio of C and S-types between NEAs and MBAs.

However, the last conclusion seems questionable because, in order to obtain the true S : C ratio among NEAs, it is necessary to divide the apparent (observed) ratio by the bias factor 5 < B(S:C) < 6. Doing this, we
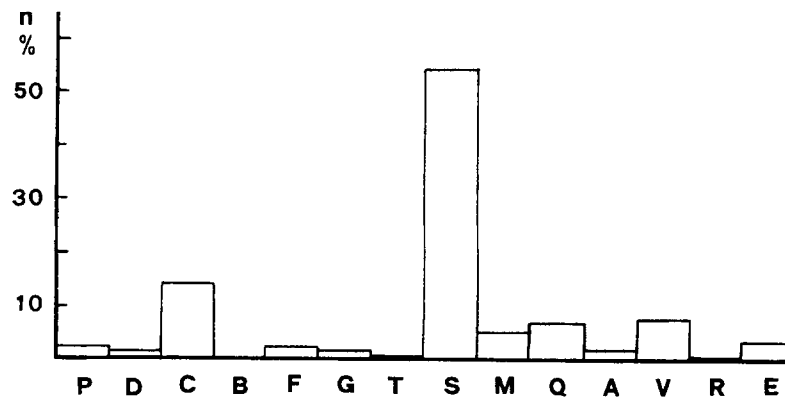
Fig. 2. Distribution of observed taxonomic classes among NEAs

obtain a corrected ratio C : S (where C includes also the different low-albedo sub-classes of the nominal C-type) of about 2, but it is well known that in the main-belt this ratio is about 5 (Zellner, 1979) or more [see the values B(S : C) for main-belt in Luu and Jewitt (1989), and the observed S : C ratio for main-belt according to Tedesco *et al.* (1989)]. So, it seems fairly likely that the relative fraction of C and other low albedo objects among NEA population is approximately 2.5 times lower than in the main asteroid belt. This could be an important constraint for the possible sources of NEA replenishment. The most immediate explanation could be that NEAs are coming preferentially from the inner regions of main-belt, where the relative abundance of C and other low albedo asteroids is lower.

Table 2 gives a brief description and a tentative mineralogical interpretation of all taxonomic classes defined by Tholen (1984) and Bell's K-class. The data presented in the Table were taken from Tholen (1984), Pieters and McFadden (1994), Tedesco and Veeder (1992), and Gaffey *et al.* (1993).

The most numerous classes observed among Aten, Apollo and Amor asteroids are S, C and V (Fig. 2). Five small V-type asteroids (3361, 3551, 3908, 4055 and 5143) in similar near-Earth orbits have reflectance spectra identical to the spectrum of the V-type MBA 4 Vesta (Binzel *et al.*, 1993a). There are two M-type asteroids (3554 Amun and 6178 1986 DA) and the results of radar observations leave no doubts on their metallic content (Tedesco and Gradie, 1987; Ostro *et al.*, 1991a). This fact seems to be very important from the point of view of possible resources in near-Earth space. There also exist representatives of the high albedo E-class (asteroid 3103 Eger, which might be a near-Earth parent body of enstatite achondrites and aubrites), of the rather rare A-class (1951 Lick, having the composition probably identical to olivine achondrites or pallasites), and of Q-class (1862 Apollo, 6611 and possibly 1864, 2368, 4688 and 1992 LR (see Binzel *et al.*, 1996)), which are believed by some authors to be the parent bodies of ordinary chondrites. The discovery of the very dark (albedo of about 0.03) and reddish D-asteroid 3552 Don Quixote among Amor objects was unexpected because asteroids of this class are mostly located in the outer-belt and in the Trojan clouds and they likely represent the most primitive asteroids in terms of composition. Don Quixote is a rather large object ($D = 19$

km) and it has an unusually elongated orbit ($a = 4.24$ AU, $e = 0.714$).

The variety of taxonomic classes discovered among NEAs indicates that this population is heterogeneous in composition and origin and is continuously mixing through dynamical evolution of the orbits (Shoemaker *et al.*, 1979; Milani *et al.*, 1989).

4. Sizes and shapes

Practically every newly discovered asteroid has a preliminary estimated diameter, derived from its photometric magnitude (extrapolated to 0˚ phase angle) and assuming an average value for the albedo. The resulting diameters are rather rough, due to the large uncertainty in the assigned asteroid albedo and magnitude-phase function. Much more accurate values of asteroid diameters can be obtained from radiometric, polarimetric, radar and other observations. Occultation and speckle interferometry measurements are only available for 433 Eros (O'Leary *et al.*, 1976; Drummond *et al.*, 1985). The methods of diameter and albedo determinations based on these techniques are described in "Asteroids II" book.

Only a few new NEA diameter determinations were obtained since the review article by McFadden *et al.* (1989) and the paper by Veeder *et al.* (1989) on radiometric determination of NEA diameters and albedos were published. The most important recent additions to the diameter data-set have been 4954 Eric ($D = 10.8$ km), 5751 Zao (6.3 km) and 2212 Hephaistos (5.7 km). On the other hand, the discovered population of NEAs has been increased by about 4 tens of very small objects (5–50 m). Amor asteroid 1036 Ganymed ($D = 38.5$ km) is still the largest NEA, two other asteroids (433 Eros and 3552 Don Quixote) are about 20 km in size, all others are not larger than 10 km and approximately 3/4 of them are less than 3 km. The smallest known NEAs are 1993 KA2 (about 6 m across, which approached the Earth in May 1993 within less than half the distance to the Moon), 1991 BA and 1991 TU (both about 6–9 m across). Among ECAs, 1627 Ivar and 1580 Betulia are the largest objects, both with diameters of about 8 km. As was already mentioned, all S and M-type asteroids larger than 6 km, and C and other low albedo types larger than 12 km are supposed to have

Table 2. Taxonomic classes, their features and interpretations

Class	Albedo	Brief description	Mineralogy meteorite analogues
P	< 0.06	Very dark and nearly neutral, featureless spectrum (identical to M, E classes), outer main-belt	Organics, anhydr. silicates
D	0.04–0.09	Dark and reddish, spectrum strongly increasing with wavelength, band at 2.2 μm is possible; outer main-belt	Kerogen-like organic material, anhydr. silicates
C	0.04–0.09	Flat-reddish spectrum, weak UV band, may have 3 μm band for hydr. silicates	Phyllosilicates, carbon. chondrites
B	0.04–0.09	C-subclass, weak UV band, reflectance decreases with wavelength, may have 3 μm band	Hydrated silicates, carbon. chondrites
F	0.04–0.09	C-subclass, weak to nonexistent UV band, may have 3 μm band	The same as B-class
G	0.06–0.10	C-subclass, strong UV band < 0.04 μm, flat vis-near IR spectrum, bands at 0.6–0.7 and 3.0 μm	Hydr. silicates phyllosilicates, carbon. chondrites
T	0.06–0.10	Broad UV–vis absorption, flat near IR spectrum	(Troilite, metal)
K	Near 0.09	S-like vis. spectrum, weak 1 μm band, flat reflectance at 1.1–2.5 μm, Eos family	Carbon CV–CO chondrites
S	0.10–0.30	UV–vis band < 0.7 μm, 1.0 μm (and or no 2.0 μm) band, red slope in vis-near IR, significant spectral variations	Pyroxene, olivine, metal
M	0.12–0.25	Featureless and reddish spectrum, near IR variations, high radar albedo	Fe-Ni metal, enstatite
Q	0.16–0.21	Strong UV band < 0.7 μm, strong absorption (olivine, pyroxene) at 1 μm, no red slope, a rare class	Ordinary chondrites
A	0.17–0.35	Strong UV and 1 μm (olivine) bands, no 2.0 μm band, a rare class	Olivine achondrites, pallasites
V	0.23–0.40	Strong UV band < 0.7 μm, 1.0 and 2.0 μm bands, weak 1.5 μm feature, a rare class	Basaltic achondrites
R	0.30–0.40	Strong UV band < 0.7 μm, 1.0 and 2.0 μm bands, red slope, a rare class	Pyroxene, olivine little (no?) metal
E	0.40–0.55	Highest albedo, featureless reddish spectrum, identical to P, M types, weak variability in near IR, inner main-belt	Enstatite achondtires, aubrites

been discovered. The absence of NEAs larger than 40 km is usually interpreted as an indication that NEAs are not primordial, but are collisional fragments of larger MBAs.

The shape of an asteroid is another fundamental characteristic related to its origin and collisional history. While large MBAs can be nearly spherical or moderately ellipsoidal, small NEAs often exhibit very irregular and elongated shapes. Information on asteroids' shapes are usually extracted from photometric lightcurves, since the lightcurve morphology is mainly caused by the changing of visible cross-sections of the rotation body. Therefore, lightcurve amplitudes are usually considered as a measure of the asteroid axial ratio (i.e. shape elongation). From numerical simulations and photometric measurements it is known that the lightcurve amplitude of a given asteroid depends on its phase angle (it increases linearly with the increasing phase angle, see Zappalà et al., 1990) and on asteroid's aspect angle (the angle between the asteroid spin vector and the line of sight). NEA amplitudes observed to date do not exceed 1.5 mag, with the exception of two Apollo asteroids: 1620 Geographos, whose amplitude measured at phase angle $\alpha = 53^{\circ}$ was 2.03 mag (Dunlap, 1974), and 1865 Cerberus, whose amplitude at a phase angle $\alpha = 21.7^{\circ}$ was 2.10 mag (Wisniewski et al., 1997). Photometric observations indicate that observed NEA amplitudes on the average are systematically larger than those of MBAs. One should take into account, however, that due to their proximity NEAs can be observed at larger phase angles, which may reach 90° and more (see, for example, 4179 Toutatis (Spencer et al., 1995), whose

lightcurves were obtained at $0.2^{\circ} < \alpha < 121^{\circ}$). At the same time, lightcurve amplitudes of MBAs are usually observed at phase angles not larger than 20°.

The question of whether the overall amplitude difference between NEAs and MBAs is caused by more elongated shapes of NEAs, or is only an effect of the different geometries of observations between NEAs and MBAs, has been clarified by Binzel et al. (1992a). They carried out a dedicated campaign of photometric observations of small MBAs and showed that there is no statistical distinction in the amplitude distributions and in the mean lightcurve amplitudes, corrected for the phase angle differences between 32 NEAs and the same number of MBAs of similar sizes (~ 3 km).

We checked this conclusion using available amplitudes for 69 NEAs and the same number of smallest MBAs. The obtained results are listed in Table 3, where "corrected amplitude" implies that mean amplitudes of NEAs and MBAs have reduced to 0° phase angle according to the empirical relation obtained by Zappalà et al. (1990). The calculations were made under the assumptions (confirmed by an analysis of observational data) that MBAs are usually observed in the phase angle range $0^{\circ}–20^{\circ}$ and NEAs in the range $5^{\circ}–60^{\circ}$. The ratio of corrected amplitudes is stable against the change of these phase angle intervals by a factor ± 1.5. Thus, the data obtained show that the apparent difference in observed amplitudes can be explained by systematic differences in phase angles. The second factor which can affect the observed amplitudes of NEAs, i.e. the aspect angle, does not seem to be important. Only 433 Eros, and possibly 1862 Apollo, were observed in

Table 3. Mean values of asteroid amplitudes and rotation rates

Population	D (km)	Observed amplitude (mag)	n	Corrected amplitude (mag)	Rotation rate (rev/day)	n
NEAs	3.7	0.55 ± 0.05	69	0.30	4.56 ± 0.33	69
MBAs	4.5	0.38 ± 0.03	69	0.28	4.56 ± 0.26	69

ranges of longitudes wide enough to include aspect angles of 90°, at which lightcurve amplitude is maximum. Almost all other NEAs were observed in short intervals of longitudes and therefore their aspect angles should be distributed around a mean value, similar to MBAs. Hence, the correction of the mean NEA lightcurve amplitude for aspect angle should be small compared to the standard deviation of the mean amplitude (Binzel *et al.*, 1992a).

A lot of qualitative new information about the shapes of NEAs was obtained during the last decade from radar observations, carried out by S. Ostro and co-workers. Approaching the Earth very closely, these objects provide a good opportunity to measure their radar echoes with a signal-to-noise ratio large enough to extract information not only about the general shape, but also about surface texture characteristics. In some cases it has been possible to obtain delay-Doppler images of the observed object.

About 40 NEAs have been observed by radar so far and the obtained data have revealed a striking diversity in shapes, from fairly symmetrical to extremely asymmetrical (Ostro *et al.*, 1988; Ostro, 1989, 1995, and other papers, see below). For example, the shape of NEAs 1917 Cuyo ($D \sim 6$ km) and 1986 JK ($D \sim 1$ km), characterized by a small elongation ($a/b \sim 1.15$ for Cuyo), are not very irregular (Ostro and Wisniewski, 1992; Ostro *et al.*, 1989). Small asteroid 6489 Golevka (1991 JX), with a maximum cross-section lower than ~ 600 m, is a highly irregular body with a pole-on elongation of 1.4 (Ostro *et al.*, 1995a). Preliminary modelling of this asteroid's shape shows that it is "dominated by large, relatively flat facets joined at sharp ridges" (Hudson and Ostro, 1995b). The same elongation and extremely irregular highly nonconvex, and possibly bifurcated shape were estimated for the 2.4 km NEA 6178 1986 DA (Ostro *et al.*, 1991a). Apollo asteroid 1685 Toro ($D = 3.4$ km) has a ratio between longest and shortest equatorial axes of 1.55 (Ostro *et al.*, 1983), but 1627 Ivar (8.1 km), and especially 433 Eros (22 km), have axial ratios of about 2.1 (Ostro *et al.*, 1990a, 1990b). So, these two rather large NEAs are more elongated than the smaller 1685 Toro, 1917 Cuyo and the much smaller 1986 JK and 6489 Golevka. The elongated shapes of NEAs may be considered as an indication of their collisional origin as fragments of large MBAs.

The convex hull of 1620 Geographos polar silhouette, estimated from an analysis of its radar echo spectra, is an evidence that this ECA is one of the most elongated and unusual objects presently known (Ostro *et al.*, 1995b). The estimates of the silhouette's extreme dimensions are 5.11 ± 0.15 km and 1.85 ± 0.15 km, corresponding to an elongation of 2.76 ± 0.21. Note that this elongation would give a zero phase angle lightcurve amplitude of 1.1 mag.

Hence, the Geographos amplitude of 2.03 mag, measured by Dunlap (1974) at $\alpha = 53°$, should be strongly affected by the geometry of the observation. Modelling the Geographos shape using the photometric lightcurves only, gives an ellipsoidal model with an elongation of 2.5–2.6 (Kwiatkowski, 1995; Magnusson *et al.*, 1996). The same elongation of Geographos shape (extreme breadths of 5.1 km and 2.0 km within 10%) is noted in another paper on radar observations of this object (Ostro *et al.*, 1996). Thus, the agreement of radar and photometric data is excellent. The pole-on silhouette of Geographos, obtained from radar observations in 1994, is irregular and non-convex and the most elongated among the Solar System objects imaged till now (Fig. 3b). The silhouette's shape seems to characterize the asteroid as a monolithic fragment derived from a disruptive collision rather than a multi-component body (Ostro *et al.*, 1995b). But 1865 Cerberus could exceed the Geographos elongation. In fact, its amplitude of 2.10 mag, measured at $\alpha = 21.7°$ (Wisniewski *et al.*, 1997) and transformed to 0° phase angle, gives an a/b axial ratio of 3.2.

The synthesised high resolution radar images of the Apollo asteroids 4179 Toutatis and 4769 Castalia (1989 PB) revealed still more exotic shapes (Hudson and Ostro, 1994; Hudson and Ostro, 1995a; Ostro *et al.*, 1995c) (Fig. 3a,c). Toutatis, which passed Earth within 0.024 AU (9.4 lunar distances) on 8 December, 1992, is a rather large object with the principal axes equal to 4.60, 2.29, and 1.92 km. Its shape is clearly bifurcated and its rotation very complex (see next section). One cannot rule out that Toutatis is a contact-binary system formed as a consequence of a gentle collision of its components (Hudson and Ostro, 1995a). The inversion of a sequence of 4769 Castalia images yielded a three dimensional model which is also strongly bifurcated and consisting of two distinct irregular km-sized lobes in contact. Castalia has dimensions $0.7 \times 1.0 \times 1.6$ km and its approximately equal lobes (with mean radii of 0.46 km and 0.40 km) are separated by a crevice 100–150 m in depth, oriented roughly perpendicularly to the asteroid longest dimension. This is the first object known among asteroids to be a fairly sure contact binary system.

Earth-approaching asteroids show a striking diversity of their shapes, from nearly spherical to very elongated and irregular, and to bifurcated and contact binaries. The opinion that NEAs have more exotic shapes than MBAs may apply only to large MBAs, because we know practically nothing about the shapes of km-sized MBAs. Though, if some small asteroids are "rubble piles", rather than single chunks of consolidated material, then a close encounter with a major planet may cause, due to the tidal
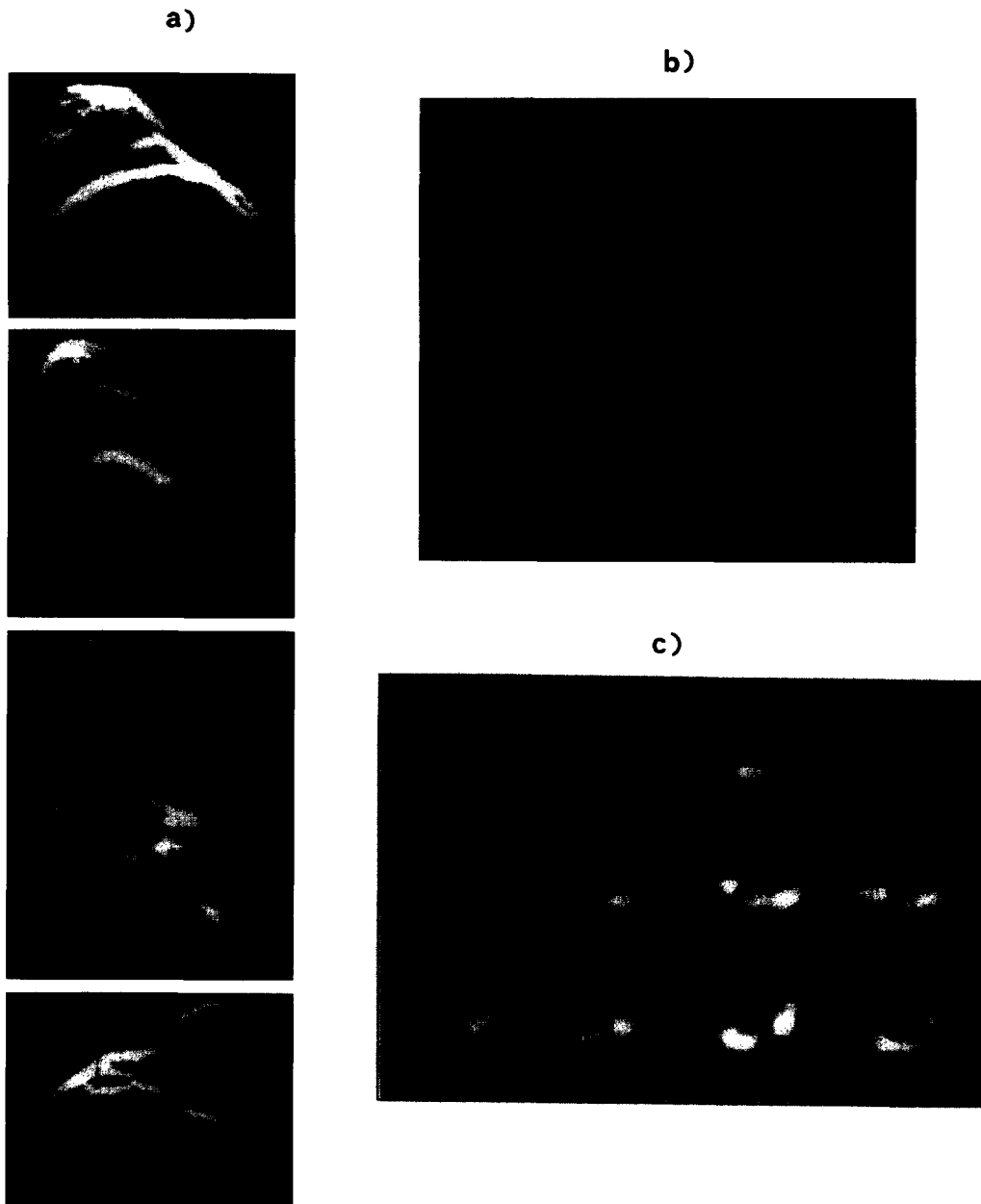
Fig. 3. The shapes of NEAs estimated from radar measurements: (a) 4179 Toutatis' radar images (Ostro *et al.*, 1995c); (b) 1620 Geographos' pole-on silhouette (Ostro *et al.*, 1995b); (c) 4769 Castalia's two-component model (Hudson and Ostro, 1994)

interactions, the object distortion into a very elongated cigar-like shape (Hills and Solem, 1994). Since close planetary approaches are possible for NEAs and not for MBAs, these shapes should be more frequent among NEAs than in the main-belt.

The relative abundance of binary systems among NEA population has relevant implications from the point of view of the collisional history of the main-belt and the delivery of material into the inner part of the Solar System (Weidenschilling et al., 1989; Martelli et al., 1993). Modelling the evolution of Earth-approaching binary asteroids (Chauvineau et al., 1995) shows that after a great number of close encounters with the Earth the binary system becomes dynamically evolved and its components may either collide (creating a contact binary configuration) or escape to infinity. The characteristic evolution time is shorter than the typical lifetime of ECAs against collisions with inner planets (~ 100 Myr). The results of numerical modelling of close encounters between binary asteroids and the Earth, obtained by Melosh and Bottke (1994), and the existence of doublet craters on the Earth and Moon confirm the abundance of double systems among the NEA population. The fraction of co-orbiting asteroids among NEAs is estimated to be about 15% (Bottke, 1996).

5. Rotation

Figure 4 shows the histogram of the distribution of the rotation rates of 69 Earth-approaching asteroids, for which this parameter is available, in comparison with the distribution of the same number of smaller MBAs. Both asteroid samples have the same means equal to 4.56 ± 0.33 and 4.56 ± 0.29 rev/day, respectively (see Table 3 in the previous section), similar dispersions and similar maxima of the rotation rate distributions (3.5–4.5 rev/day). We recall that for the whole set of MBAs the maximum of the distribution is in the range 2.0–2.5 rev/day (Binzel et al., 1989; Velichko and Lupishko, 1991). The comparison between NEAs and small MBAs (Fig. 4a, b) show that there is a small relative excess of slow rotators among NEAs, but this apparent effect might be the result of insufficient statistics and selection effects, due to the difficulties to observe small MBA. As for fast rotators, recently the rotation statistics of small MBAs has been improved by Binzel et al. (1992b) and Wisniewski et al. (1997). Their data show that among 11 fast rotators with $P \leqslant 2.60$ h, 7 asteroids belong to the Earth-approaching population and four are small MBAs. Among 26 fast rotators with $P < 3.15$ h only 12 are NEAs.

It seems reasonable to compare the rotation rate distributions of NEAs and smallest MBAs (Fig. 4a, b) with that of largest MBAs. Since the NEA population consists mainly of S-type objects and in our sample of 69 smallest MBAs it is thought that the objects of S and other moderate albedo types also predominate (due to observational selection effects), Fig. 4c shows the rotation rate distribution for the 69 largest S-type MBAs ($D > 64$ km). The maximum of this distribution corresponds to about 2 rev/day, the mean rotation rate is 2.38 ± 0.13, and its dispersion is about six times less than that of NEAs. Thus we can conclude that, on the average, NEAs rotate

practically in the same manner as the small MBAs of comparative sizes, and considerably faster than large MBAs (Binzel et al., 1989). The existence of a large fraction of fast rotators among small asteroids is not unexpected on the basis of the theories of catastrophic break-up processes and in agreement with laboratory experiments (Giblin et al., 1994), if small asteroids are really the outcomes of collisional events.

The fastest rotators among NEAs are 1566 Icarus (2.273 h), 3671 Dionysius (2.4 or 1.97 h), 1866 Sisyphus (2.40 h), and 3554 Amun (2.530 h). On the other hand, there are also NEAs rotating rather slowly, in fact five of them have rotation periods longer than 40 h, they are 3691 1982 FT (9.4 days, see Pravec, 1996a), 3102 Krok (147.8 h), 4179 Toutatis (129.84 h), 887 Alinda (73.97 h) and 2062 Aten (40.77 h). The range of rotation periods for NEAs is wider than that for the sample of small MBAs (2.35–29.25 h), and is basically the same as for all MBAs (except 288 Glauke and 1220 Crocus, whose measured periods 1150 h and 737 h, respectively, may be due to spin axis precession).

An important peculiarity of NEA rotations is that among this population three objects with very complex and non-principal axis rotation have been identified. The analysis of seven nights of photometric data of 3288 Seleucus (S-type Amor asteroid with $D \sim 3$ km) showed that a single period does not fit the observational data satisfactorily, and two or more non-harmonic frequencies are present in the lightcurve. This result allowed to conclude that Seleucus is a "tumbling" asteroid, having non-principal axis rotation (Harris, 1994b).

The second striking example of this kind is the Apollo asteroid 4179 Toutatis (Harris 1994a; Hudson and Ostro, 1995a; Spencer et al., 1995). Radar observations showed that Toutatis has an unusual rotation (Hudson and Ostro, 1995a). All three Euler angles, which describe the orientation of the body in space as a function of time, were found to be nonlinear functions of time. Toutatis' spin vector was estimated to not be parallel to the angular momentum vector or to the principal axis of inertia (that is the shortest axis). In the body-fixed coordinates Toutatis rotates around the longest axis with a period 129.8 h, and it has a long axis precession with a period of 176.4 h (Krugly et al., 1993; Spencer et al., 1995). Therefore, Toutatis' rotation is periodic only in the body-fixed coordinate system but not in an inertial one, and in general the object never repeats any given particular inertial orientation (Hudson and Ostro, 1995a). The case of Toutatis' rotation is a good confirmation of the idea that for very slow rotators the damping time scale of rotational wobble is expected to be considerably longer than the age of the Solar System, so tumbling asteroids may exist (Burns and Safronov, 1973; Harris, 1994a). Another NEA, 1994 AW1, was found to have a complex lightcurve that could be interpreted as a tumbling effect (Mottola et al., 1995a; Pravec and Hahn, 1997).

Finally, data on NEA spin vector determinations (pole coordinates, sense of rotation and sidereal period) are available only for 14 asteroids; they are collected in Table 4 and are not enough to draw any conclusion. The smallest body of the Solar System for which the axis orientation has been obtained is the Apollo asteroid 6489 Golevka with a size of about 0.6 km.

Table 4. Pole coordinates, sense of rotation, P_{sid} and shape of NEAs

Asteroid	Pole coordinates λ (deg)	β(deg)	Sense of rot.	P_{sid}[a] (day)	Shape a/b	b/c	Reference
433 Eros	29	22	P				All references for 433 Eros see Magnusson, 1989*
	4	45	—	—			
	2	53	—	—	1.79	1.18	
	−11	62	R				
	—	—	P	0.2195937			
	−7	13	I	0.21959390			
	10	46	P	0.21959386	4.0	(1.0)	
	13	28	P	—			
	17	10	—	0.21959			
	15	9	—	—	2.3		
	16	12	I	0.219599	2.6		
	—	—	—	—	4.0	1.25	
	15	20	—	—	2.33	1.00	
	23	37	P	—	2.79	1.03	
	22	9	I	0.219588			
	16	6	I	—			
1036 Ganymed	—	—	P	0.42951			Magnusson, 1989[b]
	—	—	R	—			Hahn et al., 1989
1566 Icarus	49 ÷ 299	0 ÷ 0	I	0.09471			Magnusson, 1989[b]
	214	5	I	0.094735	1.23	1.40	De Angelis, 1995
1580 Betulia	140 ÷ 320	20 ÷ 10	—	—	1.21		Magnusson, 1989[b]
	80 ÷ 212	12 ÷ 5	—	0.2565	1.7	1.4	Drummond and Wisniewski, 1990
1620 Geographos	20	−60	R	0.2176378	2.7		Magnusson, 1989[b]
	15	−77	—	0.2176366	2.7	1.05	Kwiatkowski, 1994
	54	−52	—	0.21763874	2.5	1.1	Kwiatkowski, 1995
	54	−52	R	0.21763867	2.6	1.1	Michalowski et al., 1994
	56	−47	R	0.21763866	2.58	1.00	Magnusson et al., 1996
1627 Ivar	—	—	P	0.19991			Lupishko et al., 1986
	140 ÷ 333	13 ÷ 18	P	0.199953			Velichko and Lupishkom, 1989
	110 ÷ 320	10 ÷ 40	P	0.199954			Hahn et al., 1989
1685 Toro	200	55	P	0.42481	3.2		Magnusson, 1989[b]
	220	30	P	0.424808	2.08	1.80	De Angelis, 1995
1862 Apollo	236	26	R	0.1277265			Magnusson, 1989[b]
	38	−36	R	0.127754	2.08	1.80	De Angelis, 1995
3103 Eger	—	—	P	0.2377819			Velichko et al., 1992
3908 1980 PA	177 ÷ 312	23 ÷ 61	—	0.18441	1.36	1.27	Drummond and Wisniewski, 1990
4179 Toutatis[c]	180	−52	?	—	2.01	1.19	Hudson and Ostro, 1995a, 1995b
4769 Castalia	250 ± 10	−40 ± 10	P	—	1.6	1.4	Hudson et al., 1994; Ostro et al., 1990c
6053 1003 BW3	175 ± 5	−9 + 3	—	0.1072258			Pravec 1996b
6489 Golevka	340	20	—	0.2510	a/c = 1.4		Hudson, Ostro, 1995b; Ostro et al., 1995a

[a]The accuracy of P_{sid} usually corresponds to several units of the last digit
[b]For the original references on these determinations see Magnusson (1989)
[c]Coordinates of precession axis

6. Optical properties and surface structure

The available data on the optical properties of NEAs are rather scanty and the most natural analysis is to compare them with the corresponding properties of small MBAs. Unfortunately, besides U–B and B–V color indexes, there is practically no information on other optical properties for these objects, such as polarimetric and radiometric albedos, magnitude–phase relations and polarimetric parameters. Due to their location, NEAs are also different with respect to MBAs in terms of cratering rates and flux of solar particles, both of which affect asteroid surfaces. Therefore one may expect that if differences in surface structure and optical properties between the two populations really exist they are even more prominent between NEAs and large MBAs. Since optical properties were

mostly obtained for NEAs of S-type, we will refer to a comparison with the large (> 100 km in diameter, with a mean value of 150 ± 8 km) S-type MBAs. Table 5 lists the calculated mean parameters for the two samples.

Mean albedos derived from polarimetry (Lupishko and Mohamed, 1996) and from ground-based radiometry (Morrison and Zellner, 1979; Brown et al., 1982; Brown and Morrison, 1984; Veeder et al., 1989) do not show any statistically significant difference between the two populations under scrutiny. However, both NEA albedos are a little larger than those of MBAs. If this difference is real, it may be due to the smaller contamination of S-type NEA surfaces by the matter of low albedo asteroids, as compared with the situation in the main-belt, and/or to the fact that, if the majority of NEAs are relatively young fragments, the "weathering" their surfaces have under-
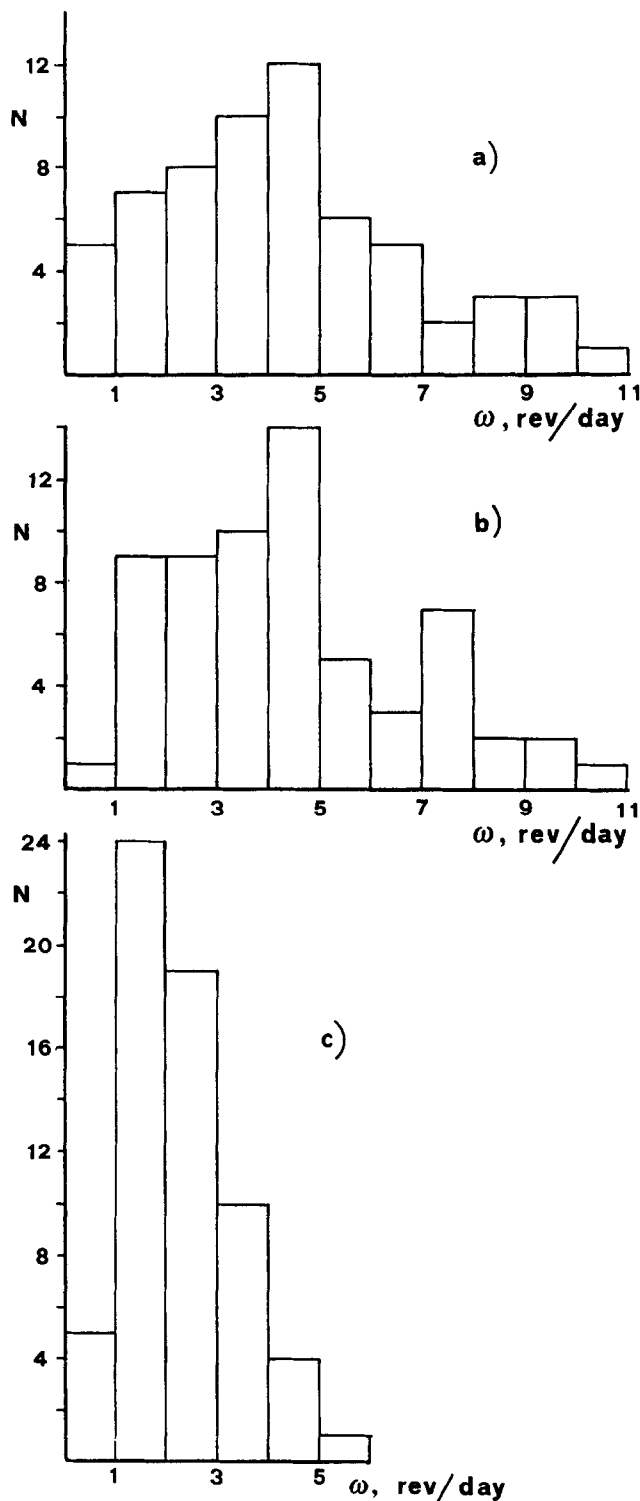
Fig. 4. Histogram distributions of rotation rates: (a) NEAs, $n = 69$, $\bar{D} = 3.5$ km, $\omega = 4.56 \pm 0.33$ rev/day; (b) MBAs, $n = 69$, $\bar{D} = 4.1$ km, $\omega = 4.56 \pm 0.29$ rev/day; (c) MBAs, $n = 69$, $\bar{D} = 116$ km, $\omega = 2.38 \pm 0.13$ rev/day

gone (Chapman, 1996) is lower. The difference in mean radiometric albedos of NEAs and MBAs as high as about 15% (Table 5) might also be due to some NEAs corresponding better to "rotating" thermophysical models, since the standard model usually overestimates the albedos of "nonstandard" asteroids. The whole range of NEA albedos is basically the same as that of MBAs, and

it corresponds to the same taxonomical class distribution among these two populations. the darkest NEA so far observed is the large D-type Amor asteroid 3552 Don Quixote with an albedo of about 0.03, while the brightest is the E-type Apollo asteroid 3103 Eger with an albedo of 0.63 (Veeder *et al.*, 1989).

The UBV colors of the relatively small NEAs and large MBAs ($D > 100$ km) also do not show appreciable differences (Table 5), although some small ($D < 50$ m) objects of the "near-Earth asteroid belt" have unusual colors (Rabinowitz *et al.*, 1993, 1994b), which are likely related to their origin (see last section).
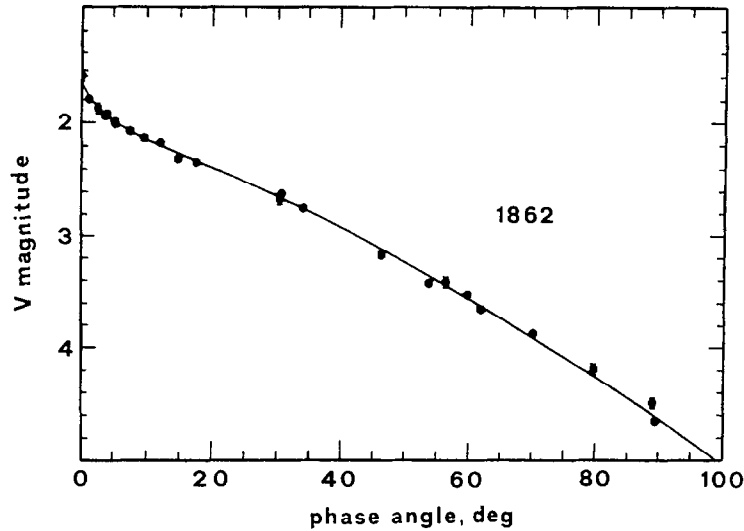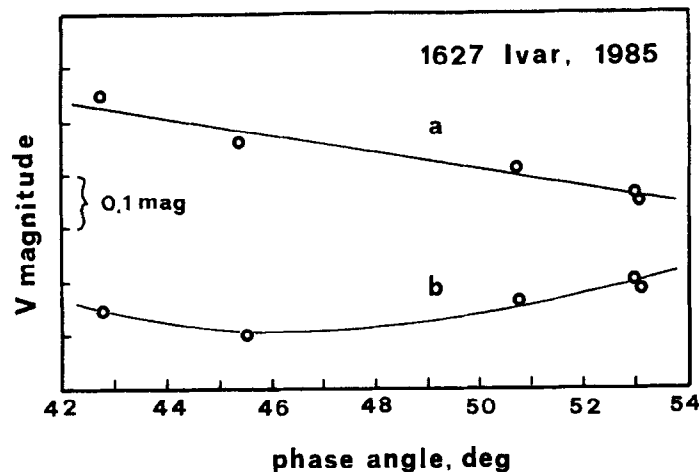
The phase dependences of magnitude, color indexes and polarization of NEAs are believed to be very useful for studying optical and structural properties of their surface because, unlike MBAs, they can be observed in a large range of phase angles (α). The phase curves of 1862 Apollo, obtained at $0.2° < \alpha < 89.4°$ (Harris *et al.*, 1987), and 4179 Toutatis ($0.2° < \alpha < 121°$, Spencer *et al.*, 1995), showed that linear approximation of asteroid magnitude–phase dependences at $\alpha > 7°–8°$, usually used for MBAs, is acceptable for phases not larger than $50°–60°$. After this limit magnitude decreases with increasing phase angle more rapidly (Fig. 5). The slope of 1862 Apollo phase curve at $\alpha = 10°$ is characterized by phase coefficient $\beta = 0.0305 \pm 0.0012$ mag/deg, which is typical of moderate albedo MBAs (Harris *et al.*, 1987).

On the other hand, the analysis of NEA magnitude–phase dependences faces a problem which practically does not exist in MBAs. This is the possible influence on the phase dependence of the aspect angle change during an opposition. Both theoretical estimates and observational data show that this effect may be very important and cannot be neglected. For instance, for S-type NEAs 1036 Ganymed and 1627 Ivar the phase coefficients were found to be equal to 0.020 ± 0.002 mag/deg and 0.017 ± 0.002 mag/deg, respectively (Lupishko *et al.*, 1986, 1988; Chernova *et al.*, 1995). These values are very small as compared with the mean value of S-type asteroids, and it is very plausible that they are affected by aspect angle changes. Figure 6 shows the observed 1627 Ivar magnitude–phase dependences at maximum of the lightcurve ($\beta = 0.017 \pm 0.002$ mag/deg) (a) and at minimum (b) (Lupishko *et al.*, 1986). The curve (b) shows an apparently strange behavior: an increase of brightness instead of the usual decrease with increasing phase angle. Calculations (using Ivar's pole coordinates given in Table 4) showed that Ivar's aspect angle changed from $41.4°$ (at $\alpha = 42.8°$) to $14.0°$ (at $\alpha = 53.2°$). Hence, during these observations the aspect angle approached the pole-on view, increasing the asteroid's brightness in spite of the phase angle change, and thereby changing appreciably Ivar's lightcurve amplitude. Figure 6 shows clearly the aspect change influence on NEAs magnitude–phase dependence.

Thus, the phase dependence of an individual NEA should not be interpreted unless the aspect–magnitude changes are taken into account. But aspect effects may be both negative and positive and statistically might not be significant. As shown in Table 5, the mean values of phase coefficients of NEAs and MBAs of S-type are also indistinguishable. Since these two asteroid populations have on average the same albedo and similar surface composition (see the next section), the strict similarity of their

Table 5. Mean optical parameters of S-type asteroids (V-band)

Parameter	NEAs ($D < 40$ km)	n	MBAs ($D > 100$ km)	n
Albedo (polarim.)	0.185 ± 0.011	9	0.177 ± 0.004	28
Albedo (radiom.)	0.190 ± 0.014	23	0.166 ± 0.006	27
U–B, mag	0.456 ± 0.012	22	0.453 ± 0.008	28
B–V, mag	0.854 ± 0.012	22	0.859 ± 0.006	28
β, mag/deg	0.029 ± 0.003	9	0.030 ± 0.006	18
P_{min}, %	0.767 ± 0.040	3	0.747 ± 0.017	28
Pol. slop, h	0.098 ± 0.006	9	0.105 ± 0.003	23
$\alpha(inv)$, deg	20.5 ± 0.2	5	20.3 ± 0.2	18

Fig. 5. Magnitude–phase dependence of 1862 Apollo obtained by Harris *et al.* (1987), taken from Helfenstein and Veverka (1989)

Fig. 6. The fragments of magnitude–phase dependences of 1627 Ivar (Lupishko *et al.*, 1986) : (a) at maximum of lightcurve, (b) at minimum

phase coefficient suggests that they should have the same porosity and surface roughness (Helfenstein and Veverka, 1989).

Parameters of NEA magnitude–phase dependences, such as the absolute magnitude H, the slope parameter G, the asteroid absolute magnitude V(1,0), obtained by extrapolating to $0°$ phase angle the linear part of the phase

curve, the phase coefficient β, and the range of covered values of phase angles, are shown in Table 6. Usually, the difference between H and V(1,0) is equal to 0.30–0.35 mag or less (Bowell *et al.*, 1985), but one can see from Table 6 that for Alinda, Icarus and Toro this difference reaches values of 0.60, 0.75 and 0.92 mag, respectively. Such large differences between extrapolated values of H and V(1,0)

Table 6. Photometric parameters of magnitude–phase dependences of NEAs

Asteroid	H (mag)	G	V (1.0) (mag)	β[a] (mag/deg)	$\Delta\alpha$ (deg)	Reference[b]
433 Eros	10.58 ± 0.03	0.370 ± 0.031	10.83 ± 0.01	0.024	8.7 ÷ 41.1	Millis et al., 1976
887 Alinda	13.15 ± 0.10	−0.265 ± 0.042	13.75 ± 0.11	0.044	16.6 ÷ 27.8	Dunlap and Taylor. 1979
1036 Ganymed	9.66 ± 0.05	0.566 ± 0.062	9.83 ± 0.02	0.020	9.6 ÷ 28.6	Chernova et al., 1995
1566 Icarus	16.04 ± 0.20	−0.017 ± 0.065	16.79 ± 0.07	0.031	38.6 ÷ 83.7	Gehrels et al., 1970
1580 Betulia	14.53 ± 0.04	0.131 ± 0.039	14.87 ± 0.03	0.034	9.1 ÷ 21.8	Tedesco et al., 1978
1620 Geographos	15.09 ± 0.06	0.31 ± 0.04	15.39 ± 0.04	0.024	10.9 ÷ 52.9	Magnusson et al., 1996
	—	—	15.21 ± 0.03	0.030	17.4 ÷ 53.2	Dunlop, 1974
1627 Ivar	12.42 ± 0.11	0.248 ± 0.079	12.82 ± 0.05	0.025	17.8 ÷ 53.9	Chernova et al., 1995
1685 Toro	12.84 ± 0.24	−0.146 ± 0.048	13.76 ± 0.13	0.038	39.2 ÷ 98.6	Dunlap, 1973
1862 Apollo	16.23 ± 0.02	0.231 ± 0.013	16.49 ± 0.02	0.030	0.2 ÷ 89.4	Harris et al., 1987
1943 Anteros	16.01 ± 0.01	0.380 ± 0.080	—	—	1.8 ÷ 21.6	Pravec et al., 1997
2100 Ra-Shalom	16.14 ± 0.18	0.165 ± 0.125	16.63 ± 0.08	0.026	27.4 ÷ 31.7	Harris et al., 1992
2212 Hephaistos	13.84 ± 0.03	0.320 ± 0.03	13.87 ± 0.08	0.023	8.0 ÷ 25.4	Pravec et al., 1997
3199 Nefertiti	15.13 ± 0.07	0.260 ± 0.06	15.46 ± 0.01	0.027	10.2 ÷ 45.8	Pravec et al., 1997
4179 Toutatis	15.30	0.10 ± 0.10	—	—	0.20 ÷ 121	Spencer et al., 1995
4954 Eric	12.37 ± 0.04	0.172 ± 0.020	12.76 ± 0.02	0.028	12.3 ÷ 60.3	Krugly and Shevchenko, 1994
5751 Zao	14.93 ± 0.07	0.190 ± 0.04	15.44 ± 0.04	0.024	20.9 ÷ 47.9	Pravec et al., 1997
6489 Golevka	19.10 ± 0.02	0.36 ± 0.07	—	—	0.2 ÷ 12	Mottola et al., 1995b
1989 VA	17.89 ± 0.01	0.15 ± 0.01	18.48 ± 0.22	0.024	27.3 ÷ 44.3	Pravec et al., 1997

[a]The errors of the phase coefficients β are equal to : 0.005 for 887 Alinda, 0.003 for 2100 Ra-Shalom and 0.002 or less for other NEAs
[b]If the referenced paper does not contain any of the parameters H, G. V(1.0) or β they were calculated by V. G. Shevchenko (Astron. Obser. of Kharkov Univ.) using original data from that paper

for these and other NEAs are due primarily to the lack of measurements at phase angles close to $0°$. As far as an extrapolation of the phase dependence to $0°$ phase angle gives a more accurate value of V(1,0) than H, one can conclude that the parameter H in such cases may be too uncertain to be used as a good estimate of an asteroid absolute magnitude.

Phase dependences of color indexes of S-type asteroids usually evidence a small reddening with increasing phase angle, but for MBAs this effect is not so evident due to the small range of phase angle during which an object is observable. Colorimetry of NEAs confirms the reddening of S and Q-type asteroids with phase angle increase and gives the following quantitative estimates of it: 1036 Ganymed : S-type; B–V : 0.0041 ± 0.0020 mag/deg; $\Delta\alpha$ = 19–28 (Chernova et al., 1995). 1862 Apollo : Q-type; U–B: 0.0024 ± 0.0007 mag/deg; $\Delta\alpha$ = 5.5–60°; B–V: 0.0026 ± 0.0004 mag/deg; $\Delta\alpha$ = 5.5–60° (Hahn, 1983).

Polarimetric parameters of NEAs, such as depth of negative polarization P_{min}, polarization slope h, and inversion angle $\alpha(inv)$, which describe the linear polarization–phase dependence and are related to surface albedo and texture, also do not differ on the average from those of large S-type MBAs (see Table 5). However, they differ noticeably from the corresponding characteristics of the

Moon and Mercury shown in Table 7 (Bowell and Zellner, 1974).

The similarity of the polarimetric parameters of NEAs and large S-type MBAs may indicate a similarity of the surface textures at submicron scales, but, in spite of the Galileo discovery that MBA 951 Gaspra (mean diameter of 12 km) is covered with a regolith of a few to several tens of meters thick (Carr et al., 1994), one cannot affirm with confidence that the surfaces of NEAs of about 1 km in size are covered with a thick regolith layer, because polarimetric data are also consistent with a solid surface coated with a thin layer of small debris (Dollfus et al., 1977).

Polarimetry of NEAs allows important information to be obtained on the polarimetric properties of the whole asteroid population (Dollfus et al., 1989b). Two S-type NEAs, 1685 Toro and 4179 Toutatis, provided a rare opportunity to observe an asteroid in a very wide range of phase angles. Polarimetric observations of Toro in 1988 at $47° < \alpha < 106°$ allowed the determination of the maximum positive polarization P_{max}, which was found to be $P_{max} = 8.5 ± 0.7\%$ at $\alpha(max) = 110° ± 10°$ (Kiselev et al., 1990). Unfortunately, the accuracy of this parameter is not high enough due to the asteroid faintness during the measurements at large phase angles. The polarimetry of Toutatis at $\alpha = 0.3–101.3°$ did not reveal any peak of

Table 7. Mean polarimetric parameters of Moon and Mercury (V band)

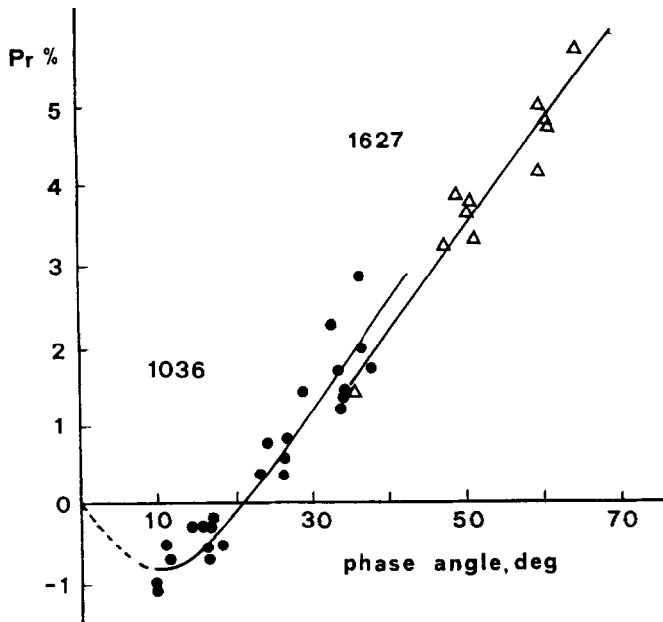|	P_{min} (%)	Pol. slope h	α_{inv} (deg)	P_{max} (%)	Albedo
Moon	1.2 ± 0.0	0.148 ± 0.005	23.6 ± 0.05	8.6	0.117
Mercury	1.4 ± 0.1	0.147 ± 0.002	25 ± 2	8.2	0.104

Fig. 7. Typical for S-asteroids polarization–phase dependences of 1036 Ganymed and 1627 Ivar (Kiselev *et al.*, 1994)

positive polarization (Mukai *et al.*, 1994). From a comparison of the Toro data and the polarization–phase dependence of 1627 Ivar (Fig. 7) it was estimated that P_{max} for Ivar should be equal to about 10–10.5% (Kiselev *et al.*, 1994). Thus, one can infer that for S-type asteroids P_{max} is close to 8.5–10.5% (to be compared with the corresponding data for Moon and Mercury in Table 7).

As it is known, P_{max} should be related to surface albedo (according to Umov's law) and particle size. On the basis of laboratory studies of the albedo dependence of P_{max} for lunar and terrestrial samples (Geake and Dollfus, 1986), the mean particle sizes of Toro and Moon regoliths have been estimated to be 30 μm and 10 μm, respectively (Kiselev *et al.*, 1990). Here the most important result is a qualitative one: the particles of Toro's regolith are considerably larger than those of the lunar regolith (Dollfus, 1989a). This result has been previously predicted from theoretical consideration on the formation of regolith on small atmosphereless bodies (Housen *et al.*, 1979) and now it has received an indirect confirmation from polarimetric data. Two S-type NEAs, 1620 Geographos and 4179 Toutatis, were observed polarimetrically in UBVRI bands and spectral dependences of polarimetric slope *h* (for Toutatis) and of inversion angle (for both asteroids) were obtained (Lupishko *et al.*, 1995; Vasilyev *et al.*, 1996). Such data exist for two asteroids only and their comparison shows that their spectral dependences of the inversion angle differ noticeably at red wavelengths (I and R bands). The observations of Toutatis revealed a new polarimetric effect unknown before. It is well-known that the position angle of the linear polarization plane of atmosphereless bodies is coplanar with the scattering plane (when $\alpha < \alpha(inv)$ and $P < 0$), or perpendicular to it (when $\alpha > \alpha(inv)$ and $P > 0$). But polarimetry of Toutatis at phase angles near the inversion point (three observations at 15.8° $< \alpha <$ 18.6°) showed that the Stokes parameter U, which corresponds to polarization with the plane of vibration oriented at an angle of 45° (or 135°) from scat-

tering plane, substantially differs from zero. Corresponding values of position angle also differ from 0° or (90°) and are near 45° (see fig. 3 in Lupishko *et al.*, 1995). This indicates the presence of polarization unconnected with the scattering plane. This effect may be related to surface heterogeneity (Lupishko *et al.*, 1995) and to the extremely complex shape of Toutatis. Similar observations of another Apollo asteroid, 1620 Geographos, also around the inversion–angle and performed with the same telescope and UBVRI polarimeter (Vasilyev *et al.*, 1996) did not show such peculiarity.

Spectral polarimetric observations of NEAs allowed another effect to be revealed (Fig. 8), which we believe also inherent to MBAs and other atmosphereless bodies. From the analysis of the wavelength dependence of S-type asteroid polarization in the phase angle range 10–90°, it was shown that the absolute value of negative polarization, measured at phase angles of about 10°, increases with wavelength, while the positive polarization (phase angles 40–90°) displays a clear decrease with increasing wavelength (Kiselev *et al.*, 1994; Lupishko and Kiselev, 1995). This indicates that an inversion of spectral dependence of S-type asteroid polarization takes place. Further observations will be able to answer the question of whether this effect can be found for S-asteroids only, or if it occurs for asteroids of different taxonomic types and for the Moon's surface as well (Lupishko and Kiselev, 1995).

Valuable information on the optical and structural properties of NEAs has been obtained from radiometric measurements of their thermal emission in the 10–20 μm wavelength range. Coupled with the data of visual photometry (asteroid absolute magnitude), radiometry gives an estimate of the visual geometric albedo and the diameter. But the results depend on the assumed thermophysical model of an asteroid (Lebofsky and Spencer, 1989). The standard (nonrotating) thermal model (nonrotating spherical asteroid with a low thermal inertia surface, i.e. with a dusty regolith) is appropriate for most NEAs and gives reasonable values of their albedos and diameters (Veeder *et al.*, 1989), which are in a good agreement with polarimetric data (see Table 8). But several objects like 1580 Betulia, 1685 Toro, 1865 Cerberus, 1915 Quetzalcoatl, 2100 Ra-Shalom, 2201 Oljato, 3199 Nefertiti, 3288 Seleucus, and perhaps 3551 Verenia and 4197 1982 TA, require a "rotating" model for a better consistency with radar (Veeder *et al.*, 1989) and polarimetric data. The "rotating" model corresponds to a sphere with a high thermal inertia surface, such as bare rock or very coarse regolith. On the average it gives asteroid albedos of about one half those given by the standard model. Modelling of 4179 Toutatis's thermophysical properties also showed that a rocky surface with little or no dust, visual albedo equal to 0.20 and thermal inertia 30–80 times that of the lunar surface, provides the best fit to near-infrared data (Howell *et al.*, 1994).

Thus, radiometry data indicate that some NEAs 0.5–5 km in sizes appear to have relatively high thermal inertia surfaces, which probably indicate large exposures of bedrock and absence of developed regolith. This does not seem dependent on asteroid size, because not only the biggest NEAs, such as Ganymed, Eros, and Ivar, satisfy well the standard model, but also small objects like 3757
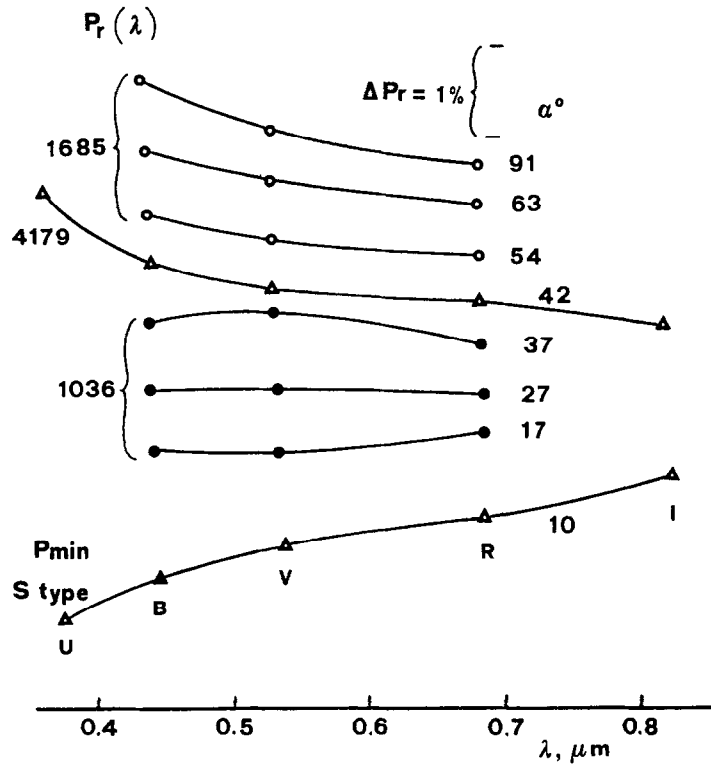
Fig. 8. Inversion effect of spectral dependence of S-type asteroid polarization (Kiselev et al., 1994)

Table 8. Polarimetric data of near-Earth asteroids (V-band)

Asteroid	P_{min} (%)	h	Inv. Angle (deg)	P_{max} (%)	pol.[a]	Albedos rad.[b]	IRAS[c]	Type	Reference to polarim. data
433	0.70	0.082	20.6	—	0.21	0.18	—	S	Morrison and Zellner, 1979
887[d]	0.76	0.095	20.0	—	0.17	0.23	—	S	Morrison and Zellner, 1979
1036	0.84	0.112	20.6	—	0.16	0.17	0.29	S	Kiselev et al., 1994
1566	—	0.082	—	—	0.22	0.42	—	S	Morrison and Zellner, 1979
1580	1.58	0.281	19.5	—	0.07	0.03	—	C	Morrison and Zellner, 1979
1620	—	0.084	20.9	—	0.21	0.19	0.33	S	Vasilyev et al., 1996
1627	—	0.131	—	(10.3)	0.14	0.12	—	S	Kiselev et al., 1994
1685	—	0.099	—	0.18	0.14	—	—	S	Kiselev et al., 1990
2062[d]	—	0.088	21.5	—	0.20	0.20	—	S	Morrison and Zellner, 1979
4179	—	0.111	20.6	—	0.16	0.20[e]	—	S	Lupishko et al., 1995

[a]Lupishko and Mohamed, 1996
[b]Veeder et al., 1989
[c]Tedesco and Veeder, 1992
[d]Transformed from B-band
[e]Howell et al., 1994

1982 XB (D = 0.5 km), 3362 Khufu (0.7 km), 2608 Seneca (0.9 km) and others.

Available radiometric data on NEAs, taken mainly from Veeder et al. (1989), are listed in Table 9.

As mentioned above, about 40 NEAs have been observed by radar at Goldstone (λ = 3.5 cm) and Arecibo (λ = 13 cm). These instruments usually transmit a circularly polarized signal and use two parallel channels to receive echoes in the same circular polarization sense as the transmitted beam (SC sense) and in the opposite sense (OC) (Ostro, 1989). The coherent single back reflection

from a dielectric interface, whose size and radius of curvature greatly exceed the signal wavelength, produces an echo with OC polarization, while SC echo can arise from multiple scattering. Therefore, the circular polarization ratio of echo powers SC/OC is a diagnostic of surface roughness within the radar wave penetration depth in the surface: if the above ratio is very low the surface should be smooth at scales of the adopted wavelength within about an order of magnitude. The second characteristic of asteroid surfaces measured by radar is the radar albedo, which is related to the bulk density, that is, to the density

Table 9. Radiometric albedos and diameters of NEAs

Asteroid	Type	Albedo (V-band)	Diameter (km)
433 Eros	S	0.18	22.0
887 Alinda	S	0.23	4.2
1036 Ganymed	S	0.17	38.5
1566 Icarus	S	0.42	0.9
1580 Betulia	C	0.03[a]	7.4[a]
1620 Geographos	S	0.19	2.0
1627 Ivar	S	0.12	8.1
1685 Toro	S	0.14[a]	5.2[a]
1862 Apollo	Q	0.21	1.5
1863 Antinous	S	0.18	1.8
1865 Cerberus	S	0.17[a]	1.2[a]
1866 Sisyphus	S	0.18	8.2
1915 Quetzalcoatl	S	0.16[a]	0.5[a]
1943 Anteros	S	0.22	1.8
1980 Tezxatlipoca	S	0.21	4.3
2062 Aten	S	0.20	0.9
2100 Ra-Shalom	C	0.08[a]	2.4[a]
2201 Oljato	S?	0.42[a]	1.4[a]
2368 Beltrovatan	SQ	0.13	2.3
2608 Seneca	S	0.16	0.9
3103 Eger	E	0.63	1.4
3199 Nefertiti	S	0.26[a]	2.2[a]
3200 Phaethon	F	0.08[a]	6.9[a]
3288 Seleucus	S	0.17[a]	2.8[a]
3360 1981 VA	—	0.10	1.8
3362 Khufu	—	0.16	0.7
3551 Verenia	V	0.28[a]	0.9[a]
3552 Don Quixote	D	0.02	18.7
3554 Amun	M	0.17	2.0
3757 1982 XB	S	0.15	0.5
4179 Toutatis	S	0.20[b]	—
4197 1982 TA	S	0.28[a]	1.8[a]
4688 1980 WF	SQ	0.18	0.6
6063 Jason	S	0.16	1.4
6178 1986 DA	M	0.12	2.3
1978 CA	S	0.06	1.9

[a] "Rotating" model
[b] Howell et al., 1994

and porosity of the surface matter. Therefore, radar observations are able to estimate some structural and physical characteristics of asteroid surfaces. Table 10 lists measured radar characteristics of NEAs.

Radar albedos are available only for three C-type NEAs and on the average they are about 1.5 times less than those of S-type objects. Most likely, this is related to the smaller bulk density and metal content of C-objects. But the mean radar albedos of small NEAs and large MBAs of the same taxonomic type, in spite of the fact that they differ in sizes about 25–50 times, are the same (Table 11). We may believe that this is due to a similar composition (mineralogy) and bulk density of both asteroid populations. If this is true, the bulk densities of C and S asteroids of similar sizes differ more than the bulk densities of the small and large asteroids of a given taxonomic class. As an alternative, the difference in radar albedo between NEAs of C and S-types is mainly due to their different metal contents. The radar albedo of the M-type Amor object 6178 1986 DA is significantly higher than that of any other asteroid observed by radar. It may in fact be a

2 km Fe-Ni object in the near-Earth space, coming from the interior of a much larger melted and differentiated parent body disrupted by a catastrophic collision (Ostro et al., 1991a).

The circular polarization ratio SC/OC of NEAs spans within about one order of magnitude (Table 10): from 0.09 (6178 1986 DA), 0.14 (1989 JA), 0.16 (1580 Betulia), to 0.78 (3908 1980 PA), 0.80 (3103 Eger) and 1.0 (2101 Adonis). This means that radar echoes of the first three asteroids are almost entirely due to single reflection from surface elements and they have much smoother surfaces at the scale of decimeters/meters than the surfaces of the latter three objects. Note that Adonis, Eger and 3908 1980 PA, with relatively rough surfaces, are about three times smaller than the former ones. However, the dependence of SC/OC ratio on asteroid diameter (Fig. 9) is rather complicated and it shows two different branches (sequences), coinciding at the upper limit of NEA diameters. This dependence needs to be explained when a larger data set on asteroids of the upper branch (radar, radiometric and optical albedos and others) becomes available.

Most NEAs appear to be covered with regolith of low thermal inertia, but the conditions of formation, accumulation and evolution of regolith on NEAs are different from those on MBAs due to the typically smaller surface gravity of NEAs, the higher flux of impactors in the main-belt (1–3 orders of magnitude, Housen and Wilkening (1982)), and the difference in the solar wind flux. As a result, the regolith of NEAs tends to be more coarse-grained than that of MBAs and still more coarse-grained than the lunar regolith. Asteroidal regoliths should be less mature than the lunar due to a more global distribution of crater ejecta and a lower magnitude of thermal effects to provide agglutinate formation. The mean topographic slope angle of macroscopic roughness (parameter θ of Hapke photometric model) has been estimated only for 1862 Apollo, and is equal to 15' (Helfenstein and Veverka, 1989), which is lower than the lunar and mercurian values (20–25'). Data in Table 11 show that SC/OC ratios of NEAs are systematically 2–3 times higher than those of large MBAs.

In conclusion, radar show that NEA surfaces are rougher than those of large MBAs at the scale length of decimeters and meters, while the porosity of NEA surface matter (for 1685 Toro it is 56% $\pm$ 12% Ostro et al., 1983) corresponds to that of the top 5–10 cm of the lunar soil (30–60%). More significantly, pronounced variations of the SC/OC ratio as a function of asteroid rotation phase suggest substantial surface heterogeneity at this roughness scale (Ostro et al., 1991a). Radar observations also show that even the relatively small NEA 4179 Toutatis seems to be cratered at about the same extent as MBAs 951 Gaspra and 243 Ida (Ostro et al., 1995c).

7. Surface composition

The variety of taxonomic classes among NEAs reflects the diversity of their surface mineralogy and an oveall analogy with the MBA population. Bell (1986) has divided Tholen's taxonomic classes (including his own K-class) into

Table 10. Radar albedos and circular polarization ratios of NEAs

Asteroid	Class	D (km)	Albedo	SC/OC	Reference
433 Eros	S	22	0.20	0.22 ± 0.06	Ostro et al., 1991a
1036 Ganymed	S	38.5	0.064	0.18 ± 0.06	Ostro et al., 1991a
1566 Icarus	S	0.9	0.16	—	Ostro et al., 1991a
1580 Betulia	C	7.4	0.09	0.16 ± 0.01	Ostro et al., 1991a
1620 Geographos	S	3.3	0.29	0.19 ± 0.05	Ostro et al., 1991a
			0.13	0.22 ± 0.01	Ostro et al., 1996
1627 Ivar	S	8.1	0.15	0.21 ± 0.01	Ostro et al., 1991a
1685 Toro	S	3.3	0.19	0.18 ± 0.04	Ostro et al., 1991a
1862 Apollo	Q	1.5	0.11	0.33 ± 0.01	Ostro et al., 1991a
1866 Sisyphus	S	8.2	0.15	0.32 ± 0.04	Ostro et al., 1991a
1915 Quetzalcoatl	S	0.5	0.10	0.27 ± 0.08	Ostro et al., 1991a
1917 Cuyo		5.7	—	0.22 ± 0.02	Ostro et al., 1991b
1981 Midas	S	3.4	—	0.65 ± 0.13	Ostro et al., 1991b
2062 Aten	S	0.9	—	0.39 ± 0.06	Benner et al., 1996
2100 Ra-Shalom	C	2.4	0.18	0.26 ± 0.02	Ostro et al., 1991a
2101 Adonis		0.6	—	1.03 ± 0.22	Benner et al., 1996
2201 Oljato	S?	1.4	—	0.31 ± 0.02	Ostro et al., 1991b
3103 Eger	E	1.5	—	0.92 ± 0.10	Benner et al., 1996
3199 Nefertiti	S	2.2	0.32	0.47 ± 0.04	Ostro et al., 1991a
3757 1982 XB	S	0.6	0.06	0.27 ± 0.05	Ostro et al., 1991a
3908 1980 PA	V	1.0	—	0.78 ± 0.02	Ostro et al., 1991b
4034 1986 PA		0.8	—	0.21 ± 0.14	Ostro et al., 1991b
4179 Toutatis	S	3.2	—	0.38 ± 0.01	De Pater et al., 1994
4544 Xanthus		1.3	—	0.25 ± 0.14	Ostro et al., 1991b
4769 Castalia	S?	1.4	0.12	0.29 ± 0.01	Ostro et al., 1991b; Hudson and Ostro, 1994
6178 1986 DA	M	2.3	0.58	0.09 ± 0.02	Ostro et al., 1991a
1986 JK	C	0.9	0.04 ÷ 0.07	0.26 ± 0.02	Ostro et al., 1989
1989 JA		1.8	—	0.14 ± 0.05	Ostro et al., 1991b
1990 MF		0.7	—	0.19 ± 0.02	Ostro et al., 1991b
1990 OS		0.4	—	0.23 ± 0.03	Ostro et al., 1991b

Table 11. Mean values of asteroid radar albedos and circular polarization ratios

Population	D (km)	n	Rad. albedo	n	SC/OC	n
NEAs, S-type	6.8 ± 2.9	14	0.16 ± 0.03	11	0.31 ± 0.04	14
MBAs, S-type	156 ± 14	10	0.15 ± 0.01	10	0.14 ± 0.02	10
NEAs, all types	4.3 ± 1.5	29	0.18 ± 0.03	16	0.34 ± 0.04	28
MBAs, all types	204 ± 36	24	0.15 ± 0.02	24	0.11 ± 0.01	22

three large superclasses distinguished by the degree of metamorphic heating they have undergone (see Table 12, taken from Gaffey et al., 1993).

The primitive objects are believed to have undergone little or no heating; the metamorphic ones have been heated sufficiently to exhibit some mineralogic alterations evidenced by their reflectance spectra; finally, the current surface mineralogy of igneous objects was formed from a melt (Bell et al., 1989). Most of the classified NEAs (~2/3) belong to the superclass of igneous objects.

Analyzing the spectra of 20 NEAs, McFadden et al. (1989) revealed a sequence of four asteroid groups in which the albedo, spectral contrast and spectral slope all increase with decreasing abundances of low-temperature assemblages and increasing abundance of high-temperature phases. Spectral data, obtained in different spectral regions (mostly in visual, but also in IR and UV), and some mineralogical characterization are available for

about 50 NEAs. These data confirm the above mentioned division of NEAs into four groups.

The low-temperature assemblages of the sequence (1st group according to the McFadden et al. (1989) classification, the typical spectrum being that of the Amor asteroid 1580 Betulia) include low-albedo asteroids of C, D, F and possibly other types (some NEAs have ambiguous classification). C asteroids have nearly featureless spectra longward of 0.4 μm, but different ultraviolet absorption bands. They apparently are formed by primitive material (mafic silicates and carbonaceous material) similar to hydrous CI and CM carbonaceous chondrite meteorites (Bell et al., 1989). The ultraviolet absorption is attributed to the presence of low-temperature hydrous phases such as phyllosilicates (clay minerals), which produce strong charge-transfer absorption bands in UV. The presence of hydrated silicates is supported by spectra of about 2/3 main-belt C-type asteroids, which exhibit an
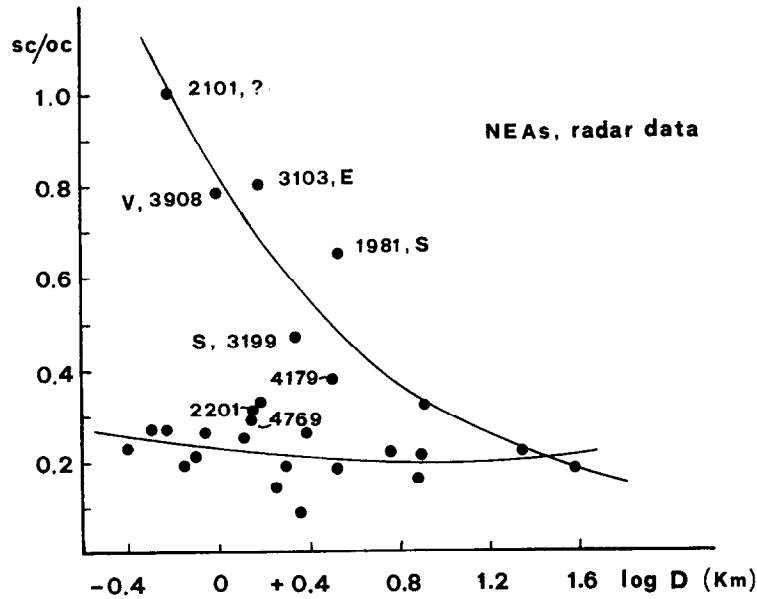
Fig. 9. Dependence of the radar circular polarization ratio SC/OC on asteroid diameter

Table 12. Bell's asteroid superclasses

Superclass	Class	Inferred minerals	Suggested meteorite analogues
Primitive	D	Clays, organics	(None)
	P	Clays, organics	(None)
	C	Clays, carbon, organics	CI and CM chondrites
	K	Olivine, pyroxene, carbon	CV and CO chondrites
Metamorphic	T	?	?
	B, G, F	Clays, opaques	Altered carbon chondrites
	Q	Pyroxene, olivine, Fe–Ni	H, L, LL chondrites
Igneous	V	Plagiocl., pyrox., olivine	Basaltic achondrites
	R	Olivine, pyroxene	Olivine-rich achondrites?
	S	Pyroxene, olivine, Fe–Ni	Pallasites, lodranites, irons
	A	Olivine	Brachinites
	M	Fe–Ni	Irons
	E	Fe-free pyroxene	Aubrites

absorption band centered around 3 μm, interpreted as diagnostic of water of hydration (Gaffey *et al.*, 1993). At present only 12 classified NEAs belong to the low-temperature group with confidence. The discovery among NEAs of the D-type asteroid 3552 Don Quixote seems to be rather exceptional because objects of this type dominate the Trojan (more than 60% of the classified objects) and Hilda groups. D asteroids have very low albedos and very red spectra longward 0.55 μm, and are believed to contain the most primitive carbonaceous-rich matter, composed of some mixture of organics, phyllosilicates and opaques (McFadden *et al.*, 1889; Gaffey *et al.*, 1993). The second compositional group of McFadden *et al.* (1989) classification also includes low-temperature assemblages, but poor in carbonaceous material, with spectra showing a strong and linear ultraviolet absorption band, moderate-to-weak 1.0 μm band (McFadden *et al.*, 1994) and moderate albedo. These parameters are similar to anhydrous CV and CO carbonaceous chondrite meteorites, which

contain less carbonaceous material and more crystalline mafic silicates, as compared to CI and CM meteorites. Typical of this group is 887 Alinda. Two other NEAs, 2100 Ra-Shalom and 3102 Krok, have similar spectra; however, the first of them has an albedo of 0.08 (Veeder *et al.*, 1989) and might represent a kind of transition between these two meteorite types (McFadden *et al.*, 1989). Still, it is worth noting that this value of Ra-Shalom's radiometric albedo was obtained with the "rotating" thermal model, but the standard one gives a moderate albedo of 0.16 (Veeder *et al.*, 1989).

The third group of moderate-temperature and carbonaceous-poor assemblages is best represented by the Q-type asteroids 1862 Apollo and 6611 1993 VW (Di Martino *et al.*, 1995). Their spectral characteristics closely correspond to those of ordinary chondrite meteorites, dominating in the present meteorite flux. The strongly reddened spectra shortward of 0.7 μm and the strong 1 μm absorptions of these Apollos indicate a piroxene-olivine

composition similar to that of ordinary chondrites, which have been exposed to temperatures ranging from 400–950°C (McSween et al., 1988). JHK photometry of Apollo implies a low Ca pyroxene (ortopyroxene) component (McFadden et al., 1985).

Due to its unique spectrum, 1862 Apollo has been classified as the only member of a separate class (Q) (Tholen, 1984). More recently, Binzel et al. (1993b) discovered the first Q-type MBA asteroid, 3628 Boznemcova (D ∼ 7 ÷ 9 km), moreover, Binzel et al. (1996) reported the results of a spectroscopic survey of NEAs in the 0.45–0.9 μm wavelength range. Out of 35 observed NEAs, six objects (2102, 5660, 1991 WA, 1993 UB, 1995 WL8 and 1995 YA3, each of them ∼3 km in diameter) have spectra similar to those of ordinary chondrite meteorites. In addition, Binzel et al. (1996) found 29 NEAs which display a continuum in the depths of the 1 μm band spanning the range between S-asteroids and ordinary chondrite meteorites. Because the spectral distribution is continuous rather than discrete, these authors concluded that Apollo-like (Q-class) asteroids are not a group really distinct from the S-class. One of the possible explanations of the close analogies between ordinary chondrites and Q-type asteroids is that these small objects are young fragments, which did not undergo weathering processes for long time. In addition to the objects quoted above, five other NEAs (1864, 2368, 3102, 4688 and 1992 LR, see Appendix) have received multiple classifications with Q-type as the most probable. Mars-crossing asteroid 2978 Nanking (D ∼ 12 km) also appears to be a good analogue for ordinary chondrites (Xu et al., 1995).

The highest-temperature assemblages, which have been heated to the melting point of silicates (about 1000°C) and differentiated, belong to the fourth NEA group in the sequence. These asteroids contain olivine and pyroxene in different proportions and a metallic component, which also is variable from one asteroid type to the other (Table 12). New and rather detailed data, related to the surface composition of one asteroid of this group, were obtained for 4179 Toutatis during its favorable opposition of 1992/1993. Combining almost simultaneous visual and near-infrared photometric and spectrophotometric data, Howell et al. (1994) have inferred that the second pyroxene absorption band of Toutatis is centered at 1.966 ± 0.012 μm, which implies an average pyroxene composition. The first piroxene band is centered at a wavelength longer than 0.96 μm, suggesting that olivine should also be present. The composite spectrum of Toutatis is very similar to those of S-type NEAs 1036 Ganymed and 1627 Ivar (Fig. 10) in overall slope and 2μm band depth. Olivine-pyroxene and possibly iron-nickel mineralogy of Toutatis is consistent with a high-temperature formation of its surface (Howell et al., 1994).

As was already mentioned, most NEAs, for which mineralogical information exists, represent differentiated assemblages. Among them there are objects with mon-omineral silicate compositions and also purely metallic ones. Small Amor asteroid 1915 Quetzalcoatl (D = 0.5 km) appears to have little or no olivine, and diogenite meteorites (Mg-pyroxenes) are the best meteorite analogous for this object (McFadden et al., 1985). Another Amor-asteroid, 3199 Nefertiti (D = 2.2 km), has the same content of pyroxene, and its mineralogical composition

corresponds to that of stony-iron meteorites, called pallasites (about 50% of Fe-Ni and the same of olivine) (Cruikshank et al., 1985). Note that Nefertiti's radar albedo (0.32) is the second highest after the M-asteroid 6178 1986 DA and more than twice as large as the mean radar albedo of S-type NEAs (see Table 10). Thus, radar data support a high metal content of 3199 Nefertiti. The only A-type NEA, 1951 Lick, also appears to have a composition identical to olivine achondrites or pallasites, and the same is true for another Amor asteroid, 4688 1980 WF, which is thought to be composed predominantly of olivine (Tholen, 1984). Lick's perihelion distance is very close to 1.3 AU, therefore it is classified sometimes as an Amor asteroid, and sometimes as a Mars-crosser. Two NEAs, 3554 Amun (Aten group) and 6178 1986 DA (Amor group), both about 2 km in size, were classified as M-types on the base of visual broadband colorimetry, JHK photometry, and 10 and 20 μm radiometry (Tedesco and Gradie, 1987). The radar measurements of 6178 1986 DA did not leave any doubt on the real metallic nature of this asteroid (Ostro et al., 1991a). Analyzing the data of the U.S. Prairie Network fireballs, in order to search for possible nickel-iron meteoroids, ReVelle and Ceplecha (1994) revealed one meteoroid to be iron in composition and to have an orbit of the Aten-type, similar to that of 3554 Amun, which may be a potential parent body of that meteoroid.

Apollo asteroid 3103 Eger is the only known E-type NEA (Veeder et al., 1989). Its high albedo (0.64), relatively neutral colors, and nearly featureless spectrum correspond to assemblages of iron-free silicate minerals, such as enstatite, forsterite, and feldspar. It is commonly believed that E-type asteroids are analogous to the enstatite achondrite meteorites (aubrites) (Bell et al., 1989; Gaffey et al., 1992). Aubrites are fragments of the crust or mantle of a parent body, composed of highly reduced materials which underwent extensive melting and magmatic differentiation, sufficient to separate most of the metal from silicates. So, aubrite parent bodies (that is, E-asteroids) must have experienced extremely strong heating up to values of at least 1,500°C (Gaffey et al., 1992). Aphelion location and mineralogy of asteroid 3103 Eger indicate that it probably derives from Hungaria region (1.9 AU) in the inner asteroid belt (Gaffey et al., 1992). This asteroid is presently in the orbital resonance 3 : 5 with the Earth and is a relatively long-lived member of the Earth-approaching population. The fall geometries of aubrites, their relatively long cosmic ray exposure ages, and the indications of a single parent body for nearly all these meteorites are in agreement with the suggestion that 3103 Eger is the unique near-Earth parent body of this meteorite type.

Five NEAs (3361, 3551, 3908, 4055 and 5143), classified as V-type (Vesta-like), have spectra nearly identical to that of main-belt V-asteroid 4 Vesta, which is known to have a differentiated structure. Their spectra (Cruikshank et al., 1991) exhibit strong first and second (1 and 2 μm) pyroxene bands and a weak band at 1.25 μm caused by traces of Fe in plagioclase feldspar. The exact wavelength positions of both pyroxene bands are sensitive to the Fe and Ca abundance in pyroxene (Adams, 1974). The pyroxene bands of 3551, 3908 and 4055 are deeper if compared to those present in the Vesta spectrum and are
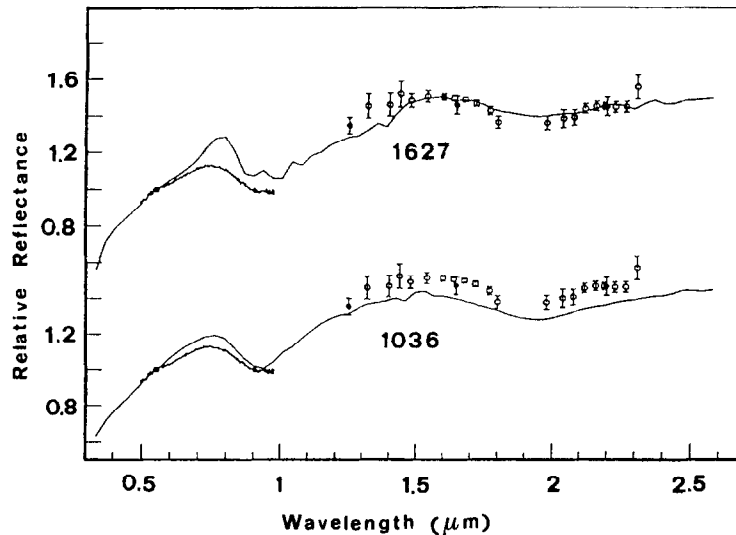
Fig. 10. The 4179 Toutatis spectrum in comparison with those of 1036 Ganymed and 1627 Ivar (solid lines) (Howell *et al.*, 1994)

consistent with more pyroxene-rich surfaces, larger grain sizes in their optically immature regoliths, more bare rock surface, or all these factors together (Cruikshank *et al.*, 1991). These NEAs are considered to have a genetic relation with Vesta and to be the possible sources of basaltic achondrite meteorites (HED-meteorites : howardites, eucrites and diogenites) (Cruikshank *et al.*, 1991 ; Binzel and Xu, 1993).

Even this brief excursus on NEA mineralogy shows that the objects of this population are very diverse in their mineralogical compositions. Taking into account their small sizes, one might infer that they are the products of much larger differentiated bodies and were injected into their present orbits from different (low- and high- temperature) zones of the Solar System.

In general, mineralogical information on NEAs, extracted from broadband photometry in different spectral regions (but mainly in visual), reflectance spectroscopy, albedo and meteorite data, seem to be poorer as compared to MBAs. Only a few NEAs were observed in the IR spectral region longward 1 μm. However, all these NEA data (especially those on S-type objects) need to be systematically analyzed together with corresponding data of MBAs. For more detailed information on NEA surface mineralogy we refer to the reader to the papers by McFadden *et al.*, 1984 ; Luu and Jewitt, 1990 ; Cruikshank *et al.*, 1991 ; Gaffey *et al.*, 1993 ; Pieters and McFadden, 1994.

8. On the NEA origin and relation to comets and meteors

The general idea on the NEA origin is that these objects are efficiently removed from other regions of Solar System by collisions and subsequent gravitational interactions with the planets on time scales of 10^6–10^8 years. Since the NEAs have unstable orbits, a continuous resupply of new objects is needed. Orbital evolution of NEAs has consequences on the geological evolution of the terrestrial

planets, as is evidenced by the existence of large craters on their surfaces. To maintain the balance between the mean rate of asteroid loss in Earth-approaching orbits and the rate of their replenishment, the latter must consist of several tens of new objects larger than 1 km in diameter over 10^6 years (Greenberg and Chapman, 1983 ; Wetherill and Chapman, 1988 ; Greenberg and Nolan, 1989).

Two main mechanisms have been commonly proposed for supplying the Earth-approaching population. The first assumes that NEAs are asteroidal fragments coming from the main-belt through collisional processes and chaotic dynamics. The results of numerical simulations show that there exist two main source locations in the main-belt : the 3 : 1 mean motion resonance with Jupiter (corresponding to the Kirkwood gap at 2.5 AU) and the inner edge of the main-belt near 2.1 AU, where the dynamics is dominated by the v_6 secular resonance (Wisdom, 1983, 1985 ; Scholl and Froeschlé, 1991). Objects orbiting in these resonant regions exhibit chaotic increases in their orbital eccentricity, allowing their orbits to cross those of terrestrial planets. In the last few years the resonance mechanisms have been analysed in more detail by Farinella *et al.* (1993, 1994), Froeschlé and Morbidelli (1994), Menichella *et al.* (1996). It was shown that secular resonances frequently play a key role. In particular, the v_6 resonance is an effective mechanism to pump up the eccentricity to $e > 0.6$ in the relatively short time of 10^6 yrs (Wisdom, 1983, 1985 ; Holman and Wisdom, 1994). Eccentricity may also reach unity (leading to collision with the Sun) when asteroids are located in overlapping resonance regions, i.e. when the object is in the secular resonance v_5 or v_6 and inside a mean motion resonance. In the region $\alpha < 2$ AU the secular resonance v_5 is also effective in pumping up the eccentricity. In addition to the dynamical modelling that supports resonance mechanisms for supplying NEAs from the main-belt, the observational data on their physical properties show that in many ways NEAs seem to resemble smaller MBAs. Almost the same taxonomic classes, an identity of reflectance spectra (McFadden *et al.*, 1985 ; Luu and Jewitt,

1990; Cruikshank et al., 1991), shape and rotation distribution (Binzel et al., 1992b; Sections 4 and 5 of this paper), and optical properties (Section 6) support the hypothesis that both populations consist primarily of fragments generated in collisions between MBAs. However, due mainly to the uncertainty in the estimates of the real abundance of the NEA population, it was not clear if all the NEAs could be supplied from the main-belt (Wetherill, 1988). But the new results of resonance mechanism modelling, obtained by Menichella et al. (1996), show that collisional evolution in the main-belt can supply a few hundreds of km-sized NEA per Myr, a sufficient rate to sustain the current population of these bodies.

The second commonly supposed source for NEAs are dormant or extinct comet nuclei; this hypothesis was originally suggested by Öpik (1963). The question about the possibility that a fraction of NEAs is actually composed by extinct comet nuclei arises from the observational evidence that some NEAs display physical and/or dynamical properties which are typically cometary (Bowell et al., 1992). When a comet nucleus has depleted its surface volatile compounds, it is believed to develop an inert mantle (crust) which effectively hides and insulates these compounds within the interior. At that point, the comet becomes inactive over a significant fraction of its surface (Weissman et al., 1989). Without the presence of an observable coma, such objects would have an asteroidal appearance and would therefore be difficult to distinguish from asteroids. Associations of the orbits of meteor streams with orbits of NEAs (Olsson-Steel, 1988; Drummond, 1991) also suggest a cometary origin for a fraction of NEAs, because the major meteor streams were previously known to be associated with active short-period comets.

Table 3 of Weissman et al. (1989) review lists nine asteroids as "strong cometary candidates" (among them 2101 Adonis, 2201 Oljato, 2212 Hephaistos, 3200 Phaethon and 3552 Don Quixote) and 20 NEAs as "possible cometary candidates". One object of the latter group, the Amor asteroid 4015 1979 VA, was found to coincide with comet P/Wilson-Harrington 1949 III (Bowell et al., 1992) and subsequently named 4015 Wilson-Harrington. The similarity between the rotation period, lightcurve amplitude, albedo and size of this object (Campins et al., 1995) with those of some other NEAs suggest that a fraction of them is of cometary origin (Osip et al., 1995). Other examples of comet–asteroid transition objects are 2060 Chiron, which was long considered as a distant asteroid and is presently classified as a comet (McFadden, 1994), and the short-period comet Parker-Hartley 1989i, which had previously been observed and catalogued as the minor planet 1968 TF (Weissman et al., 1989). NEAs 1566, 2101, 2201, 3200, 4179 and others (Babadzhanov and Obrubov, 1983; Weissman et al., 1989; Asher et al., 1993; Stohl and Porubcan, 1993) are associated with meteor streams. For the low-albedo Apollo asteroid 3200 Phaethon there can be no reasonable doubt about its association with the Geminid stream, and Phaethon could be its parent extinct comet (Fox et al., 1985). Unusual orbital, physical and mineralogical properties of another Apollo asteroid, 2201 Oljato (McFadden et al., 1993), make it, like Phaethon, one of the most plausible candidates for cometary origin. Spectral observations of 2201 Oljato, 3200 Phaethon and

4015 Wilson-Harrington, aimed at detecting a possible CN band emission at 388 μm (because this is the most easily observable indicator of cometary outgassing), showed that CN production rates for all these objects are lower (by as much as an order of magnitude) than those observed in low-active comets (Chamberlin et al., 1996). The lack of evidence of cometary activity makes it likely that 4015 now is a dormant or nearly extinct comet which had an outburst in 1949. NEAs 2201, 3200 and other "possible cometary candidates" may be analogous.

Thus, it is generally accepted that some NEAs are nuclei of extinct comets; however, the estimate of their abundance is controversial, Öpik (1963) believed that most of NEA population is composed by extinct comets. Levin and Simonenko (1981) argued against a cometary origin for most NEAs, because these are often associated with meteorites which could not have been formed in cometary nuclei. Wetherill (1988) estimated that extinct comets could provide about 40% of NEAs. Binzel et al. (1992b) constrained the fraction of comet nuclei between 0% and 40% of total NEA population. Tedesco and Gradie (1987) concluded that extinct comet nuclei are rare, if they exist at all. But at least three "asteroid–comet" objects (2060 Chiron, 4015 Wilson-Harrington and 1986 TF) are surely known. The candidates for comet nuclei should be dark objects (C, P and D-types), with average or low spin rates; they should also have unstable orbits and orbital analogy with some meteor stream. The above mentioned NEAs are the most likely candidates for cometary origin, and their physical properties satisfy these constraints.

In Section 2 it was mentioned that Spacewatch observations (University of Arizona, U.S.A) revealed an excess of small (5–50 m) objects having orbital elements similar to the Earth, which may form the "near-Earth asteroid belt" (NEAB). Regarding the possible origin of these objects, the results of collisional evolution modelling obtained by Bottke et al. (1994b) show that main-belt objects exiting the 3:1 and v_6 resonances, when they become Earth-crossing, are unlikely to become members of the NEAB group. The authors conclude that planetary ejecta from either the Earth–Moon system or Venus (but not from Mars, due to dynamical constraints) could produce an excess of these small-bodies spanning the current orbits of NEAB within 10 Myr after ejection. Moreover, Gladman and Burns (1993) found that 12 out of 15 individual orbits of small Earth-approaching asteroids are consistent with objects that were initially ejected from the Earth–Moon system on orbits having small eccentricities and inclinations.

According to Rabinowitz et al. (1993, 1994b), spectral (0.5–0.9 μm) and color (BVR) measurements of some small objects belonging to NEAB showed that their reflectance spectra and color indexes differ markedly from those of MBAs and larger Earth-approachers. Unfortunately, most of these spectra are not sampled over a wide enough wavelength range to allow comparison with meteorite spectra, but it seems plausible that small Earth-approachers originate from diverse sources. Possible sources, consistent with the analysis of orbits, are cometary debris, ejecta from the Moon, Earth, Mars, or an undiscovered population of Earth Trojans (Rabinowitz et al., 1993, 1994b).

In one of the latest papers devoted to the origin of

small Earth-approaching asteroids, Bottke *et al.* (1996b) simulated the orbital evolution of test bodies from several source regions. The results of the study show that: (a) the Earth, Moon and Venus are unlikely to provide the majority of these objects; (b) Amor asteroid fragments, evolving from low-eccentricity Mars-crossing orbits beyond a perihelion distance of 1 AU, provide the best fit to the dynamical and physical constraints of these small objects in Earth-like orbits.

9. Conclusion

It seems that the words by Tom Gehrels 26 years ago (see the first page of this review) reflect the present state of the art on NEAs. A deeper understanding of the problems raised by NEAs (especially the problem of asteroid hazard) has activated international efforts aimed at discovery and physical and dynamical studies of these objects. The new results of NEA studies allow to a better understanding of their nature, origin, and relation with comets and meteors. Indeed, their small sizes almost the same variety of taxonomic classes and reflectance spectra, the same average shapes, rotational and optical properties as compared to those of MBAs, clearly indicate the main asteroid belt as the principal source of NEA population. On the other hand, the presence of a few NEAs identifiable with extinct or dormant comets supports also a cometary origin for some of them.

In spite of the fact that NEAs are difficult targets for ground-based observations, they "help", in some sense, to study and understand the entire asteroid population. New data, like the existence of very elongated and irregular bodies (1865 Cerberus and others), contact-binary systems (4769 Castalia), bodies with very complex non-principal axis rotation and precession (3288 Seleucus and 4179 Toutatis), a complex behavior of magnitude–phase and polarization–phase dependences at large phase angles, the estimates of some optical and structural parameters of NEA surfaces, the spectral dependences of polarization-phase curve parameters, and new polarimetric effects, all shed some light on the properties of the whole asteroid population.

The study of physical properties of individual NEAs is very important not only for understanding their nature and their origin, but also for a determination of the strategy of space mission investigations of these bodies and for target selection purposes. Besides that, the physical properties of NEAs are strictly needed for the creation of an effective system of defense against their possible collisions with Earth in the framework of resolving the "asteroid hazard problem".

The discovery rate of NEAs has increased greatly over the last years, and the organization in the U.S.A. and Europe of new programs for their discovery and investigation gives good reason to hope that a new era of NEA studies will come soon. These new ground-based and space-mission investigations will give us all necessary information for the solution of fundamental and applied problems connected with NEAs.

References

Adams J. B. (1974) Visible and near-diffuse reflectance spectra of pyroxenes as applied to remote sensing of solid objects in the solar system. *J. Geophys. Res.* **79**, 4829–4836.

Asher, D. J., Clube, S. V. M. and Steel, D. I. (1993) Asteroids in the Taurid complex. *Mon. Not. R. Astron. Soc.* **264**, 93–105.

Babadzhanov, P. B. and Obrubov, Yu. V. (1993) Secular perturbations of Apollo, Amor and Aten asteroid orbits and theoretical radiants of meteor showers, probably associated with them. In *Asteroids, Comets, Meteors*, ed. C.-I. Lagerkvist, H. Rickman, pp. 411–417. Uppsala Universitet Reprocentralen.

Bell, J. F. (1986) Mineralogical evolution of asteroid belt. *Meteoritics* **2**, 333–334.

Bell, J. F., Davis, D. R., Hartmann, W. K. and Gaffey, J. J. (1989) Asteroids: the big picture. In *Asteroids II*, eds R. P. Binzel, T. Gehrels and M. S. Matthews, pp. 921–945. Univ. of Arizona Press, Tucson.

Benner, L. A., Ostro, S. J., Giorgini, J. D., Jurgens, R. F., Mitchell, D. L., Rose, R., Rosema, K. D., Slade, M. A., Winkler, R. and Yeomans, D. K. (1996) Radar observations of near-Earth asteroids 2062 Aten, 2101 Adonis, 3103 Eger, 4544 Xanthus, and 1992 QN. *Bull. Amer. Astron. Soc.*, **28**, 1105.

Binzel, R. P., Farinella, P., Zappalà, V. and Cellino, A. (1989) Asteroid rotation rates: distributions and statistics. In *Asteroids II*, ed. R. P. Binzel, T. Gehrels, M. S. Matthews, pp. 416–441. Univ. of Arizona Press, Tucson.

Binzel, R. P., Xu, S., Bus, S. J. and Bowell, E. (1992a) Origin for the near-Earth asteroids. *Science* **257**, 779–782.

Binzel, R. P., Xu, S., Bus, S. J. and Bowell, E. (1992b) Small main-belt asteroid lightcurve survey. *Icarus* **99**, 225–237.

Binzel, R. P. and Xu, S. (1993a) Chips off of asteroid 4 Vesta: Evidence for the parent body of basaltic achondrite meteorites. *Science* **260**, 186–191.

Binzel, R. P., Xu, S., Bus, S. J., Skrutskie, M. F., Meyer, M. R., Knezer, P. and Barber, E. S. (1993b) Discovery a main-belt asteroid resembling ordinary chondrite meteorites. *Science* **262**, 1541–1543.

Binzel, R. P., Bus, S. J., Burbine, T. H. and Sunshine, J. M. (1996) Spectral properties of near-Earth asteroids: Evidence for sources of ordinary chondrite meteorites. *Science* **273**, 946–948.

Bottke, W. F., Nolan, M. C., Greenberg, R., Vickery, A. M. and Melosh, H. J. (1994) Provenance of the Spacewatch small Earth-approaching asteroids. *Bull. Americ. Astron. Soc.* **26**, 1164.

Bottke, S. F. (1996) Forming binary asteroids and doublet craters with planetary tidal forces. Abstracts of "Asteroids, Comets, Meteors 96" conference, 8–12 July, 1996. Versailles, France. p. 11.

Bottke, W. F., Nolan, M. C., Melosh, H. J., Vickery, A. M. and Greenberg, R. (1996) Origin of the small Earth-approaching asteroids. *Icarus* **122**, 406–427.

Bowell, T. and Zellner, B. (1974) Polarization of asteroids and satellites. In *Planets, Stars and Nebulae Studied with Polarimetry* ed. T. Gehrels, pp. 381–404. Univ. of Arizona Press, Tucson.

Bowell, T., Harris, A. W. and Lumme, K. (1985) A two par-

ameter magnitude system for asteroids. Available in preprint form from the first author.

Bowell, E., Skiff, B. A., West, R. M., Heyer, H.-H. and Quebatte, J. (1992) (4015) 1979 VA = comet Wilson-Harrington (1949 III). *IAU Circular* 5585.

Brown, R. H. and Morrison, D. (1984) Diameters and albedos of thirty-six asteroids. *Icarus* 59, 20–24.

Brown, R. H., Morrison, D. and Telesco, C. M. (1982) Calibration of the radiometric asteroid scale using occultation diameters. *Icarus* 52, 188–195.

Burns, R. P. and Safronov, V. S. (1973) Asteroid nutation angles. *Mon. Not. R. Stron. Soc.* 165, 403–411.

Campins, H., Osip, D. J., Rieke, G. H. and Rieke, M. J. (1995) Estimates of the radius and albedo of comet-asteroid transition object 4015 Wilson-Harrington based on infrared observations. *Planet. Space Sci.* 43, 733–736.

Carr, M. H., Kirk, R. L., McEwen, A., Veverka, J., Thomas, P., Head, J. W. and Murchie, S. (1994) The geology of Gaspra. *Icarus* 107, 61–71.

Chamberlin, A. B., McFadden, L. A., Schulz, R., Schleicher, D. G. and Bus, S. J. (1996) 4015 Wilson-Harrington, 2201 Oljato and 3200 Phaethon: search for CN emission. *Icarus* 119, 173–181.

Chapman, C. R. (1996) S-type asteroids, ordinary chondrites and space weathering: The evidence from Galileo's fly-bys of Gaspra and Ida. *Meteoritics and Planetary Science* 31, 699–725.

Chapman, C. R., Harris, A. W. and Binzel R. P. (1994) Physical properties of near-Earth asteroids: implications for the hazard issue. In *Hazards Due to Comets and Asteroids* ed. T. Gherels, pp. 537–549. Univ. of Arizona Press.

Chauvineau, B., Farinella, P. and Harris, A. W. (1995) The evolution of Earth-approaching binary asteroids: a Monte Carlo dynamical model. *Icarus* 115, 36–46.

Chernova, G. P., Kiselev, N. N., Krugly, Yu. N., Lupishko, D. F., Shevchenko, V. G., Velichko, F. P. and Mohamed, R. A. (1995) Photometry of Amor asteroids 1036 Ganymed and 1627 Ivar. *Astron. J.* 110, 1875–1878.

Cruikshank, D. P., Hartmann, W. K., Tholen, D. and Bell, J. (1985) An olivine-rich Earth-crossing asteroid: Source of pallasites? *Lunar. Planet. Sci. XVI* p. 160 (abstract).

Cruikshank, D. P., Tholen, D. J., Hartmann, W. K., Bell, J. F. and Brown, R. H. (1991) Three basaltic Earth-approaching asteroids and the source of the basaltic meteorites. *Icarus* 89, 1–13.

De Angelis, G. (1995) Asteroid spin, pole and shape determination. *Planet, Space Sci.* 43, 649–682.

De Pater, I., Palmer, P., Mitchell, D. L., Ostro, S. J., Yeomans, D. K. and Snyder, L. E. (1994) Radar aperture synthesis observations of asteroids. *Icarus* 111, 489–502.

Di Martino, M., Manara, A. and Migliorini, F. (1995) 1993 VW: an ordinary chondrite-like near-Earth asteroid. *Astron. Astrophys.* 302, 609–612.

Dollufs, A., Geake, J. E., Mandeville, J. C. and Zellner, B. (1977) The nature of asteroid surfaces, from optical polarimetry. In *Comets, Asteroids, Meteorites—Interrelations, Evolutions and Origins*, ed. A. H. Delsemme, pp. 243–251. Univ. of Toledo.

Dollufs, A. (1989a) Regolith on asteroids: a polarimetric characterization. In *Asteroids, Comets, Meteors III*, eds C.-I. Lagerkvist, H. Rickman, B. A. Lindblad and M. Lindgren, pp. 49–53. Uppsala Universitet Reprocentralen.

Dollufs, A., Wolff, M., Geake, J. E., Lupishko, D. F. and Dougherty, L. (1989b) Photopolarimetry of asteroids. In *Asteroids II*, ed. R. P. Binzel, T. Gehrels, M. S. Matthews, pp. 594–616. Univ. of Arizona Press, Tucson.

Drummond, J. D. (1991) Earth-approaching asteroid streams. *Icarus* 89, 14–25.

Drummond, J. D., Cocke, W. J., Hege, E. K. and Strittmatter, P. A. (1985) Speckle interferometry of asteroids. I. 433 Eros. *Icarus* 61, 132–151.

Drummond, J. D. and Wisniewski, W. Z. (1990) The rotational poles and shapes of 1580 Betulia and 3908 (1980 PA) from one apparition. *Icarus* 83, 349–359.

Dunlap, J. L. (1973) Minor planets and related objects. IX. Photometry and polarimetry of (1685) Toro. *Astron. J.* 78, 491–501.

Dunlap, J. L. (1974) Minor planets and related objects. XV. Asteroid (1620) Geographos. *Astron. J.* 79, 324–332.

Dunlap, J. L. and Taylor, R. C. (1979) Minor planets and related objects. XXVII. Lightcurves of 887 Alinda. *Astron. J.* 84, 269–273.

Farinella, P., Gonczi, R., Froeschlé, Ch. and Froeschlé, C. (1993) The injection of asteroid fragments into resonances. *Icarus* 101, 174–187.

Farinella, P., Froeschlé, C. and Gonczi, R. (1994) Meteorite delivery and transport. In *Asteroids, Comets, Meteors* 1993 eds A. Milani, M. Di Martino and A. Cellino, pp. 205–222. Kluwer, Dordrecht.

Fox, K., Williams, I. P. and Hunt, J. (1985) The past and future of 1983 TB and its relationship to the Geminid meteor stream. In *Dynamics of Comets: their Origin and Evolution*, eds A. Carusi and G. B. Valsecchi, pp. 143–148. Reidel, Dordrecht.

Froeschlé, Ch. and Morbidelli, A. (1994) The secular resonances in the solar system. In *Asteroids, Comets, Meteors* 1993, eds A. Milani, M. Di Martino and A. Cellino, pp. 189–204. Kluwer, Dordrecht.

Gaffey, M. J., Reed, K. L. and Kelley, M. S. (1992) Relationship of E-type Apollo asteroid 3103 (1982 BB) to the enstatite achondrite meteorites and Hungaria asteroids. *Icarus* 100, 95–109.

Gaffey, M. J., Burbine, T. H. and Binzel, R. P. (1993) Asteroid spectroscopy: progress and perspectives. *Meteoritics* 28, 161–187.

Geake, J. E. and Dollfus, A. (1986) Planetary surface texture and albedo from parameter plots of optical polarization data. *Mon. Not. R. Astron. Soc.* 218, 75–91.

Gehrels, T., Roemer, E., Taylor, R. C., Zellner, B. H., Asteroid (1566) *Astron. J.* 75, 186–195. 1970.

Giblin, I., Martelli, G., Smith, P. N., Cellino, A., Di Martino, M., Zappalà, V., Farinella, P. and Paolicchi, P. (1994) Field fragmentation of macroscopic targets simulating asteroidal catastrophic collisions. *Icarus* 110, 203–224.

Gladman, B. J. and Burns, J. A. (1993) Producing small Earth approachers from lunar ejecta. *Bull. Americ. Astron. Soc.* 25, 1117.

Greenberg, R. and Chapman, C. R. (1983) Asteroids and meteorites: parent bodies and delivered samples. *Icarus* 55, 455–481.

Greenberg, R. and Nolan, M. C. (1989) Delivery of asteroids and meteorites to the inner solar system. In *Asteroids II*, ed. R. P. Binzel, T. Gehrels, M. S. Matthews, pp. 778–804. Univ. of Arizona Press, Tucson.

Hahn, G. (1983) UBVRI and JHK photometry of near-Earth asteroid 1862 Apollo. In *Asteroids, Comets, Meteors*, ed. C.-I. Lagerkvist, H. Rickman, pp. 35–44. Uppsala Universitet Reprocentralen.

Hahn, G., Magnusson, P., Harris, A. W., Young, J. W., Belkora, L. A., Fico, N. J., Lupishko, D. F., Shevchenko, V. G., Velichko, F. P., Burchi, R., Ciunci, G., Di Martino, M. and Debehogne, H. (1989) Physical studies of Apollo-Amor asteroids: UBVRI photometry of 1036 Ganymed and 1627 Ivar. *Icarus* 78, 363–381.

Harris, A. W. (1994a) Tumbling asteroids. *Icarus* 107, 209–211.

Harris, A. W. (1994b) Tumbling asteroids 2: 3288 Seleucus. *Bull. Amer. Astron. Soc.* 26, 1165.

Harris, A. W., Young, J. W., Goguen, J. et al. (1987) Photoelectric lightcurves of asteroid 1862 Apollo. *Icarus* 70, 246–256.

Harris, A. W., Young, J. W. and Dockweiler, Thor et al. (1992)

Asteroid lightcurve observations from 1981. *Icarus* **95**, 115–147.

Helfenstein, P. and Veverka, J. (1989) Physical characterization of asteroid surfaces from photometric analysis. In *Asteroids II*, ed. R. P. Binzel, T. Gehrels, M. S. Matthews, pp. 577–593. Univ. of Arizona Press, Tucson.

Hills, J. G. and Solem, J. C. (1994) Shaping of near-Earth asteroids by tidal forces. *Bull. Amer. Astron. Soc.* **26**(3), 1168.

Holman, M. and Wisdom, J. (1994) Meteorite delivery from the 3 : 1 Kirkwood gap. *Bull. Americ. Astron. Soc.* **26**, 1165.

Housen, K. R. and Wilkening, L. L. (1982) Regoliths on small bodies in the solar system. *Ann. Rev. Earth Planet. Sci.* **10**, 355–376.

Housen, K. R., Wilkening, L. L., Chapman, C. R. and Greenberg, R. J. (1979) Regolith development an evolution on asteroids and the Moon. In *Asteroids*, ed. T. Gehrels, pp. 601–627. Univ. of Arizona Press, Tucson.

Howell, E. S., Britt, D. T., Bell, J. F., Binzel, R. P. and Lebofsky, L. A. (1994) Visible and near-infrared spectral observations of 4179 Toutatis. *Icarus* **111**, 468–474.

Hudson, R. S. and Ostro, S. J. (1994) Shape of asteroid 4769 Castalia (1989 PB) from inversion of radar images. *Science* **263**, 940–943.

Hudson, R. S. and Ostro, S. J. (1995a) Shape and non-principal axis spin state of asteroid 4179 Toutatis. *Science* **270**, 84–86.

Hudson, R. S. and Ostro, S. J. (1995b) Radar-based physical models of Earth-crossing asteroids. *Bull. Amer. Astron. Soc.* **27**, 1062–1063.

Kiselev, N. N., Lupishko, D. F., Chernova, G. P. and Shkurativ, Yu. G. (1990) Polarimetry of asteroid 1985 Toro. *Kinemat. Fizika Nebesn. Tel.* **6**, 77–82 (Russian).

Kiselev, N. N., Chernova, G. P. and Lupishko, D. F. (1994) Polarimetry of asteroids 1036 Ganymed and 1627 Ivar. *Kinemat. Fizika Nebesn. Tel.* **10**, 35–39 (Russian).

Krugly, Yu. N., Velichko, F. P., Kalashnikov, A. V., Mohamed, R. A., Chiornij, V. G. and Shevchenko, V. G. (1993) UBVRI-photometry of Apollo-asteroid 4179 Toutatis. Abstracts of Science Conf. "Asteroid Hazard-93", May 25–27, 1993. St. Petersburg, p. 17.

Krugly, Yu, N. and Shevchenko, V. G. (1994) Photometry of near-Earth asteroids : 433 Eros and 4954 Eric. Abstr. of the Conf. "Small Bodies of Solar System and their Interactions with the Planets", Aug. 8–12, 1994, Mariehamn, Aland, p. 86.

Kwiatkowski, T. (1994) Physical model of 1620 Geographos, a target of the Clementine space mission. In *Dynamics and Astrometry of Natural and Artificial Celestial Bodies*, eds K. Kutzynska, F. Barlier, P. K. Sedielmann and I. Wytrzyszak, pp. 319–322. Mickiewcz Univ., Poznan.

Kwiatkowski, T. (1995) Sidereal period, pole and shape of asteroid 1620 Geographos. *Astron. Astrophys.* **294**, 274–277.

Lebofsky, L. A. and Spencer, J. R. (1989) Radiometry and thermal modeling of asteroids. In *Asteroids II* ed. R. P. Binzel, T. Gehrels, M. S. Matthews, pp. 128–147. Univ. of Arizona Press, Tucson.

Levin, B. Yu and Simonenko, A. N. (1981) On the implausibility of a cometary origin for most Apollo-Amor asteroids. *Icarus* **47**, 487–491.

Lupishko, D. F. and Kiselev, N. N. (1995) Inversion effect of spectral dependence of asteroid polarization. *Bull. Amer. Astron. Soc.* **27**, 1064.

Lupishko, D. F. and Mohamed, R. A. (1996) A new calibration of the polarimetric albedo scale of asteroids. *Icarus* **119**, 209–213.

Lupishko, D. F., Velichko, F. P. and Shevchenko, V. G. (1986) Asteroid 1627 Ivar. UBV photometry, period and sense of rotation. *Kinem. Fizika. Nebesn. Tel.* **2**, 39–43 (Russian).

Lupishko, D. F., Velichko, F. P. and Shevchenko, V. G. (1988) Photometry of Amor-asteroid 1036 Ganymed and 1139 Atami. *Astron. Vestnik* **XXII**, 167–173 (Russian).

Lupishko, D. F., Vasilyev, S. V., Efimov, Yu. S. and Shak-

hovskoj, N. M. (1995) UBVRI-polarimetry of asteroid 4179 Toutatis. *Icarus* **113**, 200–205.

Luu, J. X. and Jewitt, D. C. (1989) On the relative number of C types and S types among near-Earth asteroids. *Astron. J.* **98**, 1905–1911.

Luu, J. X. and Jewitt, D. C. (1990) Charge-coupled device spectra of asteroids. I. Near-Earth and 3 : 1 resonance asteroids. *Astron. J.* **99**, 1985–2011.

Magnusson, P. (1989) Pole determinations of asteroids. In *Asteroids II*, ed. R. P. Binzel, T. Gehrels, M. S. Matthews, pp. 1180–1190. Univ. of Arizona Press, Tucson.

Magnusson, P., Dahlgren, P., Barucci, M. A., Jorda, L., Binzel, R. P., Slivan, S. M., Blanco, C., Riccioli, D., Buratti, B. J., Colas, F., Berther, J., De Angelis, G., Di Martino, M., Dotto, E., Drummond, J. D., Fink, U., Hicks, M., Grundy, W., Wisniewski, W., Gaftonyuk, N. M., Geyer, E. H. and Bauer, T. (1996) Photometric observations and modeling of asteroid 1620 Geographos. *Icarus* **123**, 227–244.

Martelli, G., Rothwell, P., Giblin, I., Smith, P. N., Di Martino, M. and Farinella, P. (1993) Fragment jets from catastrophic break-up events and the formation of asteroid binaries and families. *Astron. Astrophys.* **271**, 315–318.

McFadden, L. A. (1994) The comet-asteroid transition : recent telescopic observations. In *Asteroids, Comets, Meteors* 1993, eds A. Milani, M. Di Martino and A. Cellino, pp. 95–110. Kluwer, Dordrecht.

McFadden, L. A., Gaffey, M. J. and McCord, T. B. (1984) Mineralogical-petrological characterization of near-Earth asteroids. *Icarus* **59**, 25–40.

McFadden, L. A., Gaffey, M. J. and McCord, T. B. (1985) Near-Earth asteroids : possible sources from reflectance spectroscopy. *Science* **229**, 160–163.

McFadden, L. A., Tholen, D. J. and Veeder, G. J. (1989) Physical properties of Aten, Apollo and Amor asteroids. In *Asteroids II*, ed. R. P. Binzel, T. Gehrels, M. S. Matthews, pp. 442–467. Univ. of Arizona Press, Tucson.

McFadden, L. A., Cochran, A. L., Barker, E. S., Cruikshank, D. P. and Hartmann, W. K. (1993) The enigmatic object 2201 Oljato : is it an asteroid or an evolved comet? *J. Geophys. Res.* **98**, 3031–3041.

McSween, H. Y., Sears, D. W. G. and Dodd, R. T. (1988) Thermal metamorphism. In *Meteorites and the Early Solar System* ed. J. F. Kerridge, M. S. Matthews, pp. 102–112. Univ. of Arizona Press, Tucson.

Melosh, H. J. and Bottke, W. F. (1994) Binary asteroids and the formation of doublet craters. *Bull. Americ. Astron. Soc.* **26**, 1167.

Menichella, M., Paolicchi, P. and Farinella, P. (1996) The main-belt as a source of near-Earth asteroids. *Earth, Moon, and Planets* **72**, 133–149.

Michalowski, T., Kwiatkowski, T., Borczyk, W. and Pych, W. (1994) CCD photometry of the asteroid 1620 Geographos. *Acta Astron.* **44**, 223–226.

Milani, A., Carpino, M., Hahn, G. and Nobili, A. M. (1989) Dynamics of planet-crossing asteroids : classes of orbital behavior. Project Spaceguard. *Icarus* **78**, 212–269.

Millis, R. L., Bowell, E. and Thompson, D. T. (1976) UBV photometry of asteroid 433 Eros. *Icarus* **28**, 53–67.

Morrison, D. (ed.) (1992) Report of the NASA Intern. Near-Earth-Object Detection Workshop, Jan. 25.

Morrison, D. and Zellner, B. H. (1979) Polarimetry and radiometry of the asteroids. In *Asteroids*, ed. T. Gehrels, pp. 1090–1097. Univ. of Arizona Press, Tucson.

Mottola, S., De Angelis, G., Di Martino, M., Erikson, A., Hahn, G. and Neukum, G. (1995a) The near-Earth objects follow-up program : first results. *Icarus* **117**, 62–70.

Mottola, S., Erikson, A., Harris, A. W., Hahn, G., Neukum, G., Buie, M. W., Sears, W. D., Harris, A. W., Tholen, D. J., Whitely, R., Magnusson, P., Piironen, J., Kwiatkowski, T., Howell, E., Hicks, M., Krugly, Yu. N., Gaftonyuk, M., Velichko, F. P., Di Martino, M., De Sanctis, G., Pravec, P.,

Fevig, R., Worman, W. and Davies, J. K. (1995b) Physical model of near-Earth asteroid (6489) 1991 JX from optical and infrared observations. *Bull. Amer. Astron. Soc.* **27**, 1055.

Mukai, T., Iwata, T., Kikuchi, S. and Mukai, S. (1994) Polarimetry of asteroids. *Planet. Space Sci.* **42**, 323–326.

O'Leary, B., Marsden, B. G., Dragon, R., Hauser, E., McGrath, M., Backus, P. and Robkoff, H. (1976) The occultation of K Geminorum by Eros. *Icarus* **28**, 133–146.

Olsson-Steel, D. (1988) Identification of meteoroid streams from Apollo asteroids in the Adelaide radar orbit surveys. *Icarus* **75**, 64–96.

Öpik, E. J. (1963) The stray bodies in the solar system. Part I. Survival of cometary nuclei and the asteroids. *Adv. Astron. Astrophys.* **2**, 219–262.

Osip, D. J., Campins, H. and Schleicher, D. G. (1995) The rotation state of 4015 Wilson-Harrington: revisiting origins for the near-Earth asteroids. *Icarus* **114**, 423–426.

Ostro, S. J. (1989) Radar observations of asteroids. In *Asteroids II*. ed. R. P. Binzel, T. Gehrels, M. S. Matthews, pp. 192–212. Univ. of Arizona Press, Tucson.

Ostro, S. J. (1995) Radar observations of near-Earth asteroids. *Spaceflight Mechanics* **89**, Advances in the Astronautical Sciences, ed. R. J. Proulx *et al.*, 869–873.

Ostro, S. J. and Wisniewski, W. Z. (1992) The shape of asteroid 1917 Cuyo. In *Asteroids, Comets, Meteors 1991*, ed. A. W. Harris, E. Bowell, pp. 447–450. Lunar and Planet. Inst., Houston.

Ostro, S. J., Campbell, D. B. and Shapiro, I. I. (1983) Radar observations of asteroid 1685 Toro. *Astron. J.* **88**, 565–576.

Ostro, S. J., Connelly, R. and Belkora L. (1988) Asteroid shapes from radar echo spectra: a new theoretical approach. *Icarus* **73**, 15–24.

Ostro, S. J., Yeomans, D. K., Chodas, P. W., Goldstein, R. M., Jurgens, R. F. and Thompson, T. W. (1989) Radar observations of asteroids 1986 JK. *Icarus* **78**, 382–394.

Ostro, S. J., Campbell, D. B., Hine, A. A., Shapiro, I. I., Chandler, J. F., Werner, C. L. and Rosema, K. D. (1990a) Radar images of asteroid 1627 Ivar. *Astron. J.* **99**(6), 2012–2018.

Ostro, S. J., Rosema, K. D. and Jurgens, R. F. (1990b) The shape of Eros. *Icarus* **84**, 334–351.

Ostro, S. J., Chandler, J. F., Hine, A. A., Rosema, K. D., Shapiro, I. I. and Yeomans, D. K. (1990c) Radar images of asteroid 1989 PB. *Science* **248**, 1523–1528.

Ostro, S. J., Campbell, D. B., Chandler, J. F., Hine, A. A., Hudson, R. S., Rosema, K. D. and Shapiro, I. I. (1991a) Asteroid 1986 DA: Radar evidence for a metallic composition. *Science* **252**, 1399–1404.

Ostro, S. J., Campbell, D. B., Chandler, J. F., Shapiro, I. I., Hine, A. A., Velez. R., Jurgens, R. F., Rosema, K. D., Winkler, R. and Yeomans, D. K. (1991b) Asteroid radar astrometry. *Astron. J.* **102**, 1490–1502.

Ostro, S. J., Choate, D., Cormier, R. A., Franck, C. R., Frye, R., Giorgini, J., Howard, D., Jurgens, R. F., Littlefair, ●, Mitchell, D. L., Rose, R., Rosema, K. D., Slade, M. A., Strobert, D. R., Winkler, R., Yeomans, D. K., Hudson, R. S., Palmer, P., Zaitsev, A., Ignatov, S., Koyama, Y. and Nakamura, A. (1995a) Asteroid 1991 JX: the 1995 Goldstone radar experiment. *Bull. Amer. Stron. Soc.* **27**, 1063.

Ostro, S. J., Rosema, K. D., Hudson, R. S., Jurgens, R. F., Giorgini, J., Winkler, R., Yeomans, D. K., Choate, D., Rose, R., Slade, M. A., Howard, S. D. and Mitchell, D. L. (1995b) Extreme elongation of asteroid 1620 Geographos from radar images. *Nature* **375**, 474–477.

Ostro, S. J., Hudson, R. S., Jurgens, R. F., Rosema, K. D., Campbell, D. B., Yeomans, D. K., Chandler, J. F., Giorgini, J. D., Winkler, R., Rose, R., Howard, S. D., Slade, M. A., Perillat, P. and Shapiro, I. I. (1995c) Radar images of asteroid 4179 Toutatis. *Science* **270**, 80–83.

Ostro, S. J., Jurgens, R. F., Rosema, K. D., Hudson, R. S., Giorgini, J. D., Winkler, R., Yeomans, D. K., Choate, D., Rose, R., Slade, M. A., Howard, S. D., Scheeres, D. J. and

Mitchell, D. L. (1996) Radar observations of asteroid 1620 Geographos. *Icarus* **121**, 46–66.

Pieters, C. M. and McFadden, L. A. (1994) Meteorite and asteroid reflectance spectroscopy: clues to early solar system processes. *Ann. Rev. Earth Planet. Sci* **22**, 457–497.

Pravec, P. (1996a) Slow rotation of (3691) 1982 FT. Abstracts of "Asteroids, Comets, Meteors 1996" conference, 8–12 July, 1996, Versailles, France, p. 36.

Pravec, P. (1996b) Pole solution from single long-lasting apparition of a NEA: the case of (6053). Abstracts of "Asteroids, Comets, Meteors 96" conference, 8–12 July, 1996, Versailles, France, p. 45.

Pravec, P. and Hahn, G. (1997) Two-period lightcurve of 1996 AW1: Indication of a binary asteroid? *Icarus*, submitted.

Pravec, P., Wolf, M., Sauronova, L., Mottola, S., Erikson, A., Hahn, G., Harris, A. W., Harris, A. W. and Young J. W. (1997) The near-Earth follow-up program II. Results for 8 asteroids from 1982 to 1995. *Icarus*, submitted.

Rabinowitz, D. L. (1994) The size and shape of the near-Earth asteroid belt. *Icarus* **111**, 364–377.

Rabinowitz, D. L., Gehrels, T., Scotti, J. V. *et al.* (1993) Evidence for a near-Earth asteroid belt. *Nature* **363**, 704–706.

Rabinowitz, D. L., Bowell, E., Shoemaker, E. and Muinonen, K. (1994a) The population of Earth-crossing asteroids. In *Hazards Due to Comets and Asteroids*, ed. T. Gehrels, pp. 285–312. Univ. of Arizona Press, Tucson.

Rabinowitz, D., Howell, E. and Hicks, M. (1994b) Unusual colors for small Earth approachers. *Bull. Amer. Astron. Soc.* **26**, 1173.

ReVelle, D. O. and Ceplecha, Z. (1994) Analysis of identified iron meteoroids: possible relation with M-type Earth-crossing asteroids? *Astron. Astrophys.* **292**, 330–336.

Scholl, H. and Froeschlé, Ch. (1991) The v_6 secular resonance region near 2 AU: a possible source of meteorites. *Astron. Astrophys.* **245**, 316–321.

Shoemaker, E. M., Williams, J. G., Helin, E. F. and Wolf, R. F. (1979) Earth-crossing asteroids: orbital classes, collision rates with Earth, and origin. In *Asteroids*, ed. T. Gehrels, pp. 253–282. Univ. of Arizona Press, Tucson.

Shoemaker, E. M., Wolf, R. F. and Shoemaker, C. S. (1990) Asteroid and comet flux in the neighborhood of Earth. *Geol. Soc. of America*, Special Paper 247, 155–170.

Spencer, J. R., Akimov, L. A., Angeli, C., Angelini, P., Barucci, M. A., Birch, P., Blanco, C., Buie, M. W., Caruso, A., Chiornij, V. G., Colas, F., Dentchev, P., Dorokhov, N. I., De Sanctis, M. C., Dotto, E., Ezhkova, O. B., Fulchignoni, M., Green, S., Harris, A. W., Howell, E. S., Hudecek, T., Kalashnikov, A. V., Kobelev, V. V., Korobova, Z. B., Koshin, N. I., Kozhevnikov, V. P., Krugly, Yu. N., Lazzaro, D., Lecacheux, J., MacConnell, J., Mel'nikov, S. Y., Michalowski, T., Mueller, B. E. A., Nakamura, T., Neese, C., Nolan, M. C., Osborn, W., Pravec, P., Riccioli, D., Shevchenko, V. S., Shevchenko, V. G., Tholen, D. J., Velichko, F. P., Venditti, C., Venditti, R., Wisniewski, W., Young, J. and Zellner, B. (1995) The lightcurve of 4179 Toutatis: evidence for complex rotation. *Icarus* **117**, 71–89.

Stohl, J. and Porubcan, V. (1993) Complexes of the associated meteoroids, asteroids and comets. Asteroids, comets, meteors 1993, Belgirate, Italy, June 14–18, 1993, p. 283.

Tedesco, E., Drummond, J., Candy, M., Birch, P., Nikoloff, I. and Zellner, B. (1978) 1580 Betulia: An unusual asteroid with an extraordinary lightcurve. *Icarus* **35**, 344–359.

Tedesco, E. F. and Gradie, J. (1987) Discovery of M class objects among the near-Earth asteroid population. *Astron. J.* **93**, 738–745.

Tedesco, E. F. and Veeder, G. J. (1992) IMPS albedo and diameter catalog (FP 102). In *Infrared Astronomical Satellite Minor Planet Survey Catalog*, ed. E. F. Tedesco, pp. 243–295. Phillips Laboratory Technical Report NO. PL-TR-92-2049. Hanscom Air Force Base, MA.

Tedesco, E. F., Williams, J. F., Matson, D. L., Veeder, G. J.,

Gradie, J. C. and Lebofsky, L. A. (1989) Three-parameter asteroid taxonomy classifications. In *Asteroids II*, eds R. P. Binzel, T. Gehrels and M. S. Matthews, pp. 1151-1161. Univ. of Arizona Press, Tucson.

Tholen, D. J. (1984) Asteroid taxonomy from cluster analysis of photometry. Ph.D. Thesis, Univ. of Arizona.

Vasilyev, S. V., Lupishko, D. F., Shakhovskoj, N. M. and Efimov, J. S. (1996) UBVRI polarimetry and photometry of asteroid 1620 Geographos. *Kinem. Fizika Nebevsn. Tel.* **12**, 13-18 (Russian).

Veeder, G. J., Hanner, M. S., Matson, D. L. and Tedesco, E. F. (1989) Radiometry of near-Earth asteroids. *Astron. J.* **97**, 1211-1219.

Velichko, F. P. and Lupishko, D. F. (1989) Photometric astronomy for Earth-approaching asteroids : the pole coordinates of 1627 Ivar. *Kinem. Fizika Nebesn. Tel.* **5**, 90-94 (Russian).

Velichko, F. P. and Lupishko, D. F. (1991) Asteroid rotation (review). *Astron. Vestnik* **25**, 259-276 (Russian).

Velichko, F. P., Krugly, Y. N. and Chiornij, V. G. (1992) Sidereal rotational period of Apollo-asteroid 3103 1982 BB. *Astron. Tsirk.* 1553, 37-38 (Russian).

Weidenschilling, S. J., Paolicchi, P. and Zappalà, V. (1989) Do asteroids have satellites? In *Asteroids II* ed. R. P. Binzel, T. Gehrels, M. S. Matthews, pp. 643-658. Univ. of Arizona Press, Tucson.

Weissman, P. R., A'Hearn, M. F., McFadden, L. A. and Rick-

man, H. (1989) Evolution of comets into asteroids. In *Asteroids II*, ed. R. P. Binzel, T. Gehrels, M. S. Matthews, pp. 880-920. Univ. of Arizona Press, Tucson.

Wetherill, G. W. (1988) Where do Apollo objects come from? *Icarus* **76**, 1-18.

Wetherill, G. W. and Chapman, C. R. (1988) Asteroids and meteorites. In *Meteorites and the Early Solar System*, ed. J. F. Kerridge, M. S. Matthews, pp. 35-67. Univ. of Arizona Press, Tucson.

Wisdom, J. (1983) Chaotic behavior and the origin of the 3/1 Kirkwood gap. *Icarus* **56**, 51-74.

Wisdom, J. (1985) Meteorites may follow a chaotic route to earth. *Nature* **315**, 731-733.

Wisniewski, W. Z., Michalowski, T. M., Harris, A. W. and McMillan, R. S. (1997) Photometric observations of 125 asteroids. *Icarus* **126**, 395-449.

Xu, S., Binzel, R. P., Burbine, T. H. and Bus, S. J. (1995) Small main-belt asteroid spectroscopic survey : initial results. *Icarus* **115**, 1-35.

Zappalà, V., Cellino, A., Barucci, M. A., Fulchignoni, M. and Lupishko, D. F. (1990) An analysis of the amplitude-phase relationship among asteroids. *Astron. Astrophys.* **231**, 548-560.

Zellner, B. (1979) Asteroid taxonomy and the distribution of the compositional types. In *Asteroids*, ed. T. Gehrels, pp. 783-806. Univ. of Arizona Press, Tucson.

Appendix. Physical parameters of near-Earth asteroids

Asteroid	Group	H (mag)	Albedo[a]	Diam. (km)	Cl.	Period (hrs)	Ampl. (mag)	U–B	B–V	Radar Obs.[b]
433 Eros	Am	10.75	0.12	22	S	5.270	0.05–1.5	0.53	0.93	2
887 Alinda	Am	13.76	0.23	4.2	S	73.97	0.35	0.44	0.93	
1036 Ganymed	Am	9.45	0.19	39	S	10.31	0.12–0.45	0.42	0.84	1
1221 Amor	Am	17.70	m	1.0				0.1		
1566 Icarus	Ap	16.40	0.22	1.5	S	2.273	0.05–0.22	0.52	0.77	2
1580 Betulia	Am	14.52	0.08	5.8	C	6.132	0.21–0.65	0.25	0.66	2
1620 Geographos	Ap	15.60	0.25	2.0	S	5.223	1.10–2.03	0.47	0.86	2
1627 Ivar	Am	13.20	0.14	8.1	S	4.797	0.25–1.0	0.46	0.87	1
1685 Toro	Ap	14.23	0.31	3.4	S	10.196	0.6–0.8	0.47	0.88	3
1862 Apollo	Ap	16.23	0.25	1.5	Q	3.065	0.15–0.60	0.48	0.82	1
1863 Antinous	Ap	15.54	0.24	2.1	S	4.02	0.12	0.36	0.76	
1864 Daedalus	Ap	14.85	m	3.7	SQ	8.57	0.85	0.50	0.83	
1865 Cerberus	Ap	16.84	0.22	1.2	S	6.810	1.48–2.10	0.44	0.79	
1866 Sisyphus	Ap	13.00	0.16	8.2	S	2.402	0.11	0.45	0.88	1
1915 Quetzalcoatl	Am	18.97	0.21	0.5	S	4.9	0.26	0.43	0.78	1
1916 Boreas	Am	14.93	m	3.5	S			0.41	0.85	
1917 Cuyo	Am	13.90	m	5.7		2.691	0.44			1
1943 Anteros	Am	15.75	0.17	2.3	S	>3	0.17	0.44	0.84	
1951 Lick	Am	14.70	m	3.9	A	4.424	0.27	0.57	1.04	
1980 Tezcatlipoca	Am	13.85	0.25	4.3	S	7.250	0.95	0.46	0.96	
1981 Midas	Ap	15.00	m	3.4	S	5.220	0.65	0.48	0.97	2
2061 Anza	Am	16.56	d	2.6	TCG	11.50	0.3	0.35	0.83	
2062 Aten	At	16.80	0.26	1.1	S	40.77	0.26	0.46	0.93	1
2100 Ra-Shalom	At	16.05	0.08	3.4	C	19.79	0.34	0.31	0.71	2
2102 Tantalus	Ap	15.30	m	3.3		2.391	0.07–0.09			
2201 Oljato	Ap	15.55	0.33	1.9	S	24	>0.1	0.38	0.83	1
2212 Hephaistos	Ap	13.84	m	5.7	SG	>20	0.08–0.11	0.40	0.77	
2340 Hathor	At	20.26	m	0.3	CSU			0.50	0.77	
2368 Beltrovata	Am	15.21	0.27	2.3	SQ	5.9	1.05	0.52	0.83	
2608 Seneca	Am	17.52	0.21	0.9	S	8	0.5	0.45	0.83	
3102 Krok	Am	16.70	m	1.6	QRS	147.8	>1.0	0.52	0.83	
3103 Eger	Ap	15.21	0.64	1.5	E	5.709	0.72–0.9	0.24	0.73	3

Asteroid	Group	H (mag)	Albedo[a]	Diam. (km)	Cl.	Period (hrs)	Ampl. (mag)	U–B	B–V	Radar Obs.[b]
3122 Florence	Ap	14.20	m	4.9		5	0.20			
3199 Nefertiti	Am	15.13	0.42	2.2	S	3.021	0.12	0.42	0.90	1
3200 Phaethon	Ap	14.60	0.09	6.9	F	3.604	0.12			
3288 Seleucus	Am	15.00	0.22	2.8	S	>16	>0.4	0.50	0.91	
3360 1981 VA	Ap	16.20	0.17	1.8						
3361 Orpheus	Ap	19.03	mv	0.4	V	3.58	0.32	0.50	1.02	
3362 Khufu	At	18.10	0.21	0.7			>0.14			
3551 Verenia	Am	16.81	0.37	0.9	V	4.930	0.11–0.15	0.48	0.84	
3552 Don Quixote	Am	13.00	0.03	19.0	D	7.7	>0.41			
3554 Amun	At	15.82	0.20	2.0	M	2.530	0.19	0.24	0.71	
3671 Dionysius	Ap	16.30	m	1.9		2.4	0.26			
3691 1982 FT	Am	14.50	m	4.3		226	0.55	0.44		
3753 1986 TO	At	14.40	m	4.5		27.4	0.95			
3757 1982 XB	Am	18.95	0.18	0.5	S	9.012	0.20	0.52	0.86	1
3908 1980 PA	Am	17.30	0.23	1.0	V	4.426	0.25–0.46			1
3988 1986 LA	Am	18.30	m	0.7		8	0.2			
4015 Wilson-Harrington	Ap	15.99	0.05	2.0	CF	6.1	0.2	0.28	0.67	
4055 Magellan	Am	14.50	0.23	3.4	V	7.5	0.5	0.43		
4179 Toutatis	Ap	14.00	0.13	3.2	S	129.8	1.1	0.51	0.86	1
4197 1982 TA	Ap	15.40	0.15	2.8	S	3.540	0.29			
4660 Nereus	Ap	18.30	m	0.7	C					
4688 1980 WF	Am	18.60	0.18	0.6	SQ					
4769 Castalia	Ap	16.90	m	1.4		4.086	1.0	0.46	0.93	1
4953 1990 MU	Ap	14.30	m	3.6	S	14.218	>0.70			
4954 Eric	Am	12.50	m	10.8	S	12.065	0.59	0.42	0.85	
5143 Heracles	Ap	13.90	mv	3.0	V					
5332 1990 DA	Am	14.90	m	3.6	S	5.803	0.37			
5370 Taranis	Am	15.90	0.05	4.4	C		0.02			
5646 1990 TR	Am	14.50	m	4.3	S	6.25	0.19			
5653 1992 WD5	Am	15.40	m	3.2		4.834	0.85			
5751 Zao	Am	14.93	m	6.3		>21.7	0.00–0.12			
5797 1980 AA	Am	19.40	m	0.4	S	2.706	0.12–0.17	0.37	0.81	
5836 1993 MF	Am	15.00	m	3.8		4.959	0.53–0.76			
6053 1993 BW3	Am	14.60	m	4.1		2.573				
6063 Jason	Ap	16.60	0.21	1.4	S		0.16			
6178 1986 DA	Am	15.90	0.15	2.3	M	3.58	0.32	0.27	0.68	1
6322 1991 CQ	Am	16.30	m	2.10		4.323	0.70			
6489 Golevka	Ap	19.10	m	0.6		6.027	0.4–1			1
6491 1991 OA	Am	16.92	m	0.7		2.69	0.08			
6611 1993 VW	Ap	16.50	m	1.9	Q					
1977 VA	Am	19.40	m	0.4	XC			0.21	0.71	
1978 CA	Ap	16.90	0.09	1.9	S	3.756	0.8	0.48	0.91	
1986 JK	Ap	18.90	0.05	0.9	C		0.05	0.49	0.68	1
1987 PA	Am	18.40	m	0.7	C					
1988 TA	Ap	20.90	d	0.4	C					
1989 DA	Ap	17.90	m	0.9		3.925	0.12			
1989 UP	Ap	20.60	m	0.3		6.96	1.16			
1989 VA	At	17.89	m	1.0		2.514	0.22–0.40			
1989 VB	Ap	20.00	m	0.4		16	>0.32			
1990 HA	Ap	16.70	m	1.4		8.55	>0.08			
1990 KA	Am	16.00	m	2.3		6	0.5			
1990 OA	Am	17.10	m	1.4		5	1.2			
1990 SA	Am	17.00	m	1.4	S					
1990 UA	Ap	19.40	m	0.4		long	0.08			
1990 UP	Am	20.50	m	0.3		20	0.8			
1991 EE	Ap	17.50	m	1.0		3.057	0.14–0.38			1
1991 VA (L)	Ap	27.00	m	0.017			0.40			
1991 VK	Ap	17.00	m	1.4	S					
1991 WA	Ap	16.90	m	1.6	S					
1991 XB	Am	18.10	m	0.9	SX					
1992 LR	Am	18.00	m	1.0	Q					
1992 NA	Am	16.50	m	1.9	C					
1992 CC1	Ap	15.00	m	3.8	S					
1992 TC	Am	18.30	m	1.0	X	5.540	0.07			
1992 UB	Am	16.00	m	2.2	X					

Asteroid	Group	H (mag)	Albedo[a]	Diam. (km)	Cl.	Period (hrs)	Ampl. (mag)	U–B	B–V	Radar Obs.[b]
1993 BX3	Ap	20.80	m	0.3		20.463	0.91			
1993 KA	Ap	26.00	m	0.028	CX					
1993 QP	Am	17.50	m	1.2		24				
1994 AW1	Am	17.60	m	1.2		11.198	>0.35			
1995 EK1	Ap	16.92	m	1.4		8.444	0.45			
1995 FI	Ap	20.61	m	0.3		9.2	0.30			

[a] When albedo not measured but inferred from taxonomic class, it is listed as 'd' for "dark" (0.06), 'm' for "medium" (0.15), 'mv' for "mean for V-type" (0.30)

[b] In the last column the number of apparitions for which successful radar observations have been obtained is given

(L) following asteroid number means that object's orbit is not sufficiently secure and probably asteroid is lost

"X" is E, M or P-type, which have very similar spectra